Biomaterials

DOI: 10.1002/anie.201404272

The Mechanical Role of Metal Ions in Biogenic Protein-Based Materials

*Elena Degtyar, Matthew J. Harrington, Yael Politi, and Peter Fratzl**

Keywords:
adhesives · biomaterials · metal coordination · sacrificial bonds · self-healing materials

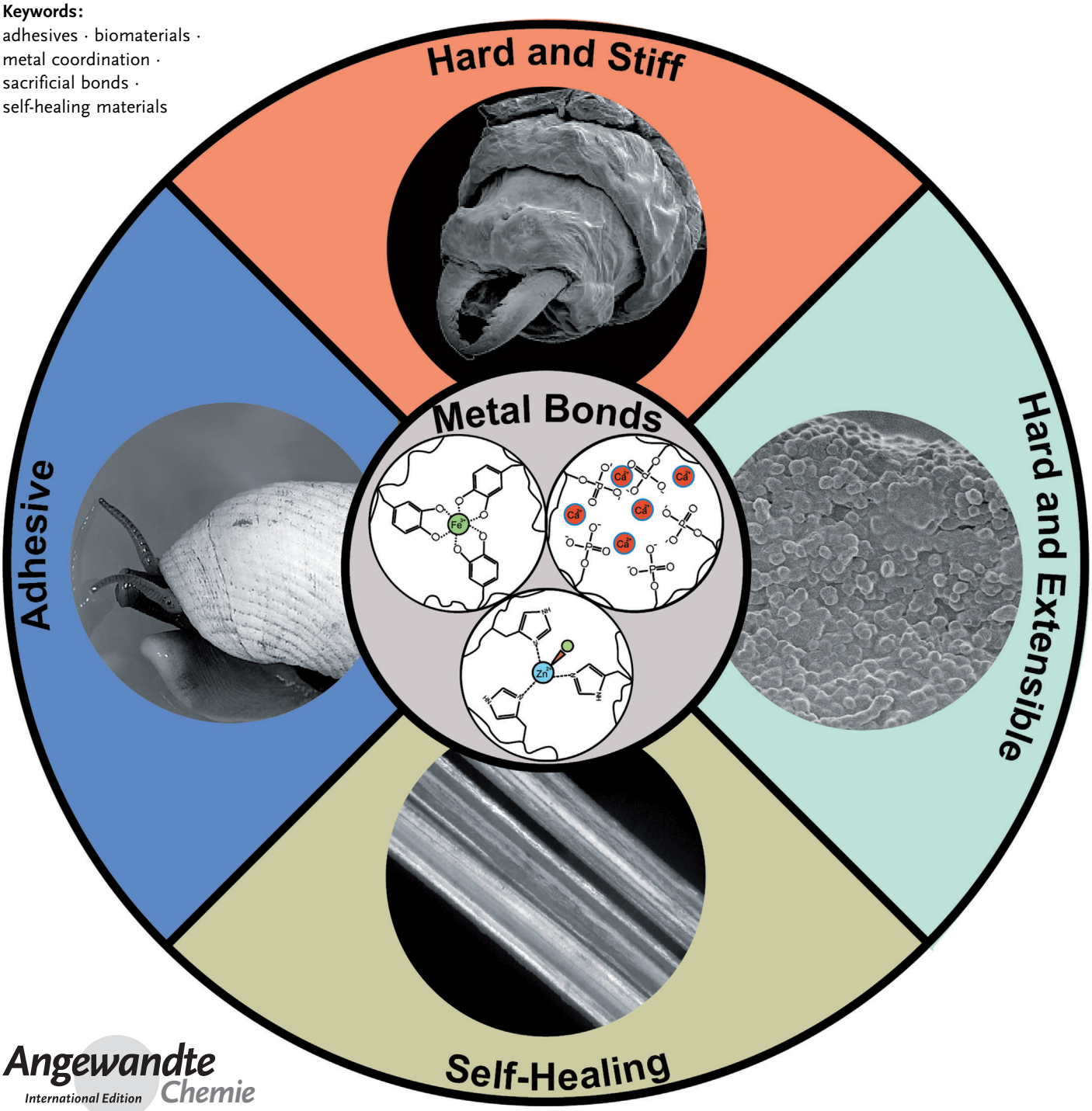

Angewandte International Edition Chemie

Protein-metal interactions—traditionally regarded for roles in metabolic processes—are now known to enhance the performance of certain biogenic materials, influencing properties such as hardness, toughness, adhesion, and self-healing. Design principles elucidated through thorough study of such materials are yielding vital insights for the design of biomimetic metallopolymers with industrial and biomedical applications. Recent advances in the understanding of the biological structure–function relationships are highlighted here with a specific focus on materials such as arthropod biting parts, mussel byssal threads, and sandcastle worm cement.

From the Contents

1. Introduction

Metal coordination bonds, also referred to as coordinate covalent bonds, are a unique class of chemical interactions that straddle the normally distinct line between covalent and non-covalent bonding. The biological metal coordination interactions between large biomolecules (especially proteins) and common transition metal ions (e.g., Fe, Zn, Cu, and Ni) have been mostly studied in the context of their roles in essential physiological functions such as catalysis, gas transport, electron transfer, metal scavenging, and signal transduction[1] (Figure 1). However, more recently, metal coordination complexes have also been identified in protein-based biological materials in which they contribute to important survival functions such as adhesion, load-bearing, abrasion resistance, and protection from predators, thereby endowing materials with increased toughness, hardness, and even autonomic and intrinsic self-healing properties (Figure 1). These studies have prompted an interest in adapting the principles extracted from such metal-doped biological materials for the development of bioinspired metallopolymers that attempt to harness some of these behaviors for technological and biomedical applications.[2–5]

The overarching aim of the present Review is to emphasize and highlight the diversity of mechanical functions and properties existing in biogenic materials (i.e., materials produced by living organisms) possessing protein–metal coordination bonds as well as to provide an overview of the current mechanistic understanding of the structure–function relationships that define these materials and of the biological processing steps instrumental to their formation. Biogenic materials consist of assemblies of a relatively limited selection of molecular building blocks, which belong to several classes of large biomolecules synthesized in the living cells (e.g., proteins, lipids, and carbohydrates), as well as small molecules (e.g., vitamins and cofactors) and ions scavenged from the environment. The fine-tuning of material properties is further achieved by a rich variety of intermolecular physical interactions bridging the building blocks. Thus, the blending of organic and inorganic components in different relative amounts and the biological control over hierarchical structure across length scales results in a large variety of emergent properties that are linked to the adaptive fitness of the organism.[6–8]

In the context of biogenic materials, protein–metal coordination bonds serve as bridging bonds in a variety of different materials (see Figure 1); however, as will become clear throughout this Review, this method of cross-linking offers several advantages to the achievement of unique material properties: 1) metal–ligand coordinate covalent bonds are typically weaker than covalent bonds given that they deviate from the "classical" covalent definition due to the fact that both electrons comprising the bond come from the same donor. Nonetheless, these bonds are stronger than other types of non-covalent bonds (e.g. hydrogen bonds); 2) metal–ligand bonds are kinetically labile, allowing them to reform on short time scales; 3) metal–ligand bonds are highly directional, thus the stereochemical and coordination symmetry of a metal can be utilized for imposing hierarchical structure onto a biomaterial;[9,10] 4) metal coordination can be formed or broken through pH changes or external ligands, a feature extensively exploited in the formation of biological materials (discussed at detail in Section 6). Figure 1 provides a sampling of the types of bonds and materials that will be discussed and provides a guideline for the structure of the Review. First, a quick general introduction to metalloproteins will be followed by a more specific examination of typical metal coordination complexes found in nature (Figure 1, left and middle panels). The Review then moves to a detailed examination of specific examples of materials, in which protein–metal coordination is employed to achieve a wide

[*] Dr. E. Degtyar, Dr. M. J. Harrington, Dr. Y. Politi, Prof. P. Fratzl
Max Planck Institute of Colloids and Interfaces
Department of Biomaterials
Research Campus Golm, 14424 Potsdam (Germany)
E-mail: peter.fratzl@mpikg.mpg.de

range of mechanical functions (Figure 1, right panel). This is followed by a brief discussion of the relevant processing and assembly mechanisms for the construction of such materials. Whereas the focus of the review is primarily biological and biochemical, efforts are made to emphasize current endeavors by researchers to generate bioinspired metallopolymers based on these natural systems.[4,11–14]

2. Metals and Ligands in Metalloproteins

Based on recent genomics and proteomics data, an estimated third of all proteins in living organisms require metal cofactors for their function.[15] Enzymes, in particular, rely on the unique properties of metal–ligand complexes to catalyze the fundamental biological processes of respiration, photosynthesis, and nitrogen fixation, among others.[16–18] Metal coordination bonds occur when a chemical group or groups act as ligands by donating lone pairs of electrons to the metal ion empty orbitals. In protein–metal coordination the environment of such complexes is extended beyond that including the metal core and the coordinating ligands, for example, the secondary coordination shell comprised of residues interacting with the ligands at a distance less than 3.5 Å.[19] Typical metal ions coordinated by proteins include Zn, Cu, Fe, Ca, Mg, and Mn, but others are also possible. In principle, main chain carbonyl and amino groups from all amino acids are able to participate in metal bonding under certain conditions;[20,21] however, in practice, only some of the 21 proteogenic amino acids are able to function as ligands: for example, side chain hydroxy groups (serine (Ser), threonine (Thr), and tyrosine (Tyr)), carboxylate groups (aspartic acid (Asp) and glutamic acid (Glu)), the imidazole group of histidine (His), as well as thiol and thioether groups (cysteine (Cys) and methionine (Met)). In addition to standard amino acids, selective post-translational modifications (PTM) of specific amino acid side chains can serve as strong ligands for metal ions, especially 3,4-dihydroxyphenylalanine (DOPA), phosphoserine (pSer), and several others.[2,22] Noteworthy, although out of the scope of this review, are non-protein organic cofactors that chelate metal ions in biology such as the heme in oxygenases,[23] bacterial siderophores[24] (Figure 1), chlorophylls,[25] and several others. Finally, secondary-shell amino acid residues that interact with the primary ligands (e.g., through hydrogen bonding) can have important effects on the structural and chemical nature of the protein–metal interaction including the thermodynamic stability and kinetic dissociation rate of the complex, the pK_a values of ligand groups, and the oxidation state and redox potential of the metal center.[26–28]

Metal coordination bonds are traditionally recognized for their physiologically important properties, such as the catalytic function of enzymes; however, they are also extremely relevant to the mechanical performance of many biogenic materials. These bonds stand out in comparison to the typical bonding strategies, such as covalent and non-covalent interactions. Covalent bonding in protein assemblies offers high strength and thermodynamic stability, and thus, functions as

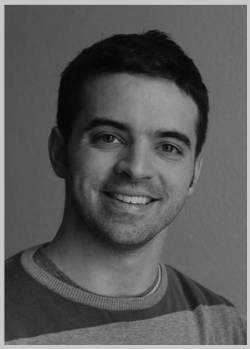

Matthew J. Harrington received his Ph.D. in the lab of J. Herbert Waite from the University of California, Santa Barbara. This was followed by a Humboldt postdoctoral fellowship at the Max Planck Institute of Colloids and Interfaces in the department of biomaterials, where he is currently a research group leader. His research is focused on understanding biochemical structure–function relationships in protein-based biological materials with a specific focus on the role of metal coordination bonds in mechanics and assembly processes.

Elena Degtyar has received her Ph.D. in 2009 in the Department of Microbiology and Molecular Biotechnology from Tel Aviv University, Israel. In 2011 she started her postdoctoral research in the department of Biomaterials in MPI for Colloids and Interfaces (Potsdam, Germany) in the group of Matthew J. Harrington focusing on recombinant protein-based bioinspired materials. Among her research interests are mechanical properties of recombinant metal-reinforced protein-based structures. In 2013 she received funding for studying importance of liquid crystal phase in the process of mussel byssus thread formation as part of the Promotion of Young Researchers in the SPP1568 program.

Yael Politi studied biology at Tel Aviv University and received her Ph.D. in 2009 from the faculty of chemistry at the Weizmann Institute of Science, Rehovot, after performing her research under the supervision of Prof. Lia Addadi and Prof. Steve Weiner. She then moved to the Max Planck Institute of Colloids and Interfaces in the department of biomaterials as a Humboldt postdoctoral fellow, where she is currently a research group leader. Her research group is studying structure–function relationships in chitin-based biological materials and sensors.

Peter Fratzl is director at the Max Planck Institute of Colloids and Interfaces in Potsdam, Germany, and honorary professor at the Humboldt University Berlin and Potsdam University. He holds an engineering degree from Ecole Polytechnique in Paris, France, and a doctorate in Physics from the University of Vienna, Austria. His scientific interests include the relation between structure and mechanical behavior of biological and bioinspired composite materials and he has published more than 400 research papers. Peter Fratzl is Fellow of the Austrian Academy of Sciences, of the German Academy of Science and Engineering, and of the Materials Research Society (USA). He holds an honorary doctorate from the University of Montpellier and is recipient of the Leibniz Prize from the German Science Foundation.

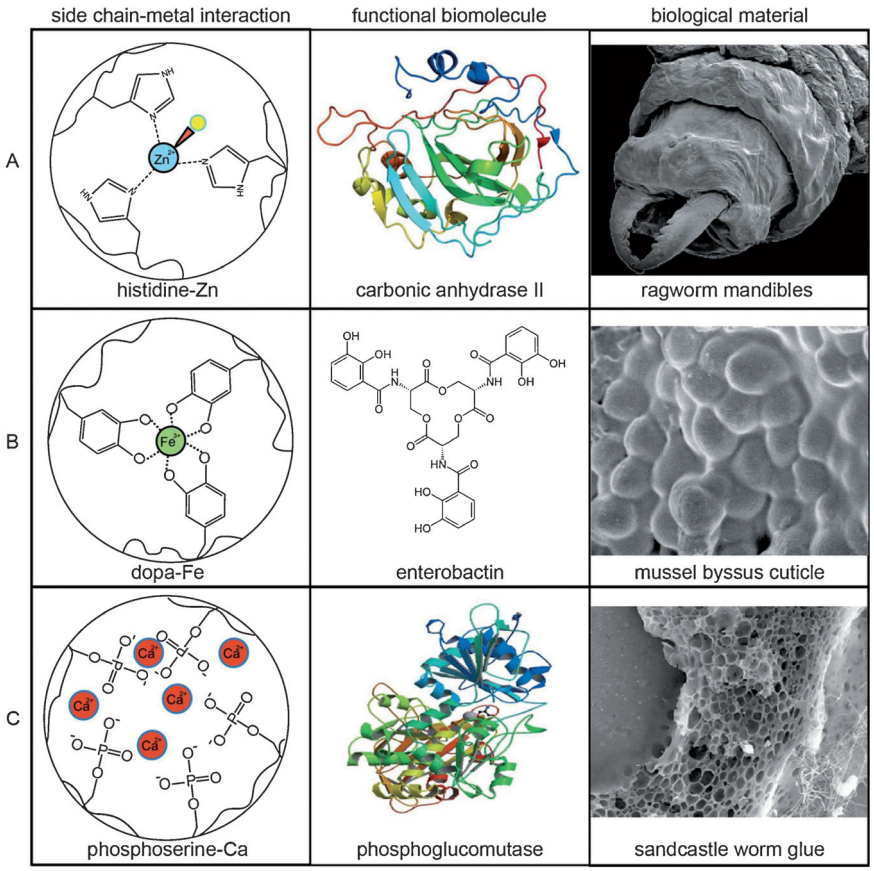

Figure 1. Biochemical and mechanical functional roles of biological metal coordination bonds. Amino acid side chain interactions with metal ions provide functionalities to biomolecules such as the enzymes carbonic anhydrase (A) (PDB No. 12ca)[182] and phosphoglucomutase (C) (PDB No. 1VKL)[183] as well as in metal scavenging siderophores, such as enterobactin (B).[184] These same interactions also behave as load-bearing cross-links, for example, in the hardening of marine worm mandibles[93] (A) (SEM image of Ragworm mandibles is reprinted with permission from [72]. Copyright 2008; American Chemical Society.); the hard and extensible behavior of mussel byssus cuticle[50] (B) and the adhesive properties of sandcastle worm glue (C). SEM image is reproduced with permission from [125].

an essentially permanent cross-linking strategy. Conversely, non-covalent interactions, such as hydrogen bonds are more transient and possess much lower binding energies. Nonetheless, these weaker bonds are employed prodigiously in biological materials, for example, to cooperatively stabilize load-bearing secondary structures.[29] On the scale of bond strengths, protein–metal interactions can possess strengths of up to about half of a covalent bond;[30] however, these bonds are quite labile and the kinetics of bond dissociation and re-association can range over many orders of magnitude. In fact, fundamental studies on metallopolymers have demonstrated that the slow dissociation kinetics, rather than bond energy, is linked to material mechanical properties, in this case stiffness, whereas fast reformation of bonds following mechanical rupture has been implicated in material healing.[31,32] Thus, one main advantage of metal coordination bonding in the context of biological materials is the high bond strength combined with reversibility and fast re-association kinetics. As we will see, these features are extensively exploited in biological materials with load-bearing functions (e.g., mussel byssal threads and slug slime). Biological organisms, as opposed to inorganic chemists, are comparatively limited in their selection of metals and ligands. For example, a Ru- or Pt-based enzyme metal center is highly unlikely owing to the relative scarcity of these metals in the environment.[33] Additionally, there is a limited selection of suitable ligands in proteins as they are restricted to the 21 naturally occurring amino acids and a selection of PTMs. In spite of these apparent limitations, the functions for which combinations of metals and ligands have emerged throughout evolutionary history are diverse.

A main determinant for the complexing strength of a metal ion is its polarizability, which is essentially the ratio of charge to ionic radius. Due to increased nuclear charge, alkali metals interact with ligands more weakly than the alkaline earth cations like Ca^{2+} and Mg^{2+}. The same applies to divalent cations of the first transition series that decrease in size from left to right along the periodic table ($Mn^{2+} > Fe^{2+} > Co^{2+} > Ni^{2+} > Cu^{2+} > Zn^{2+}$). Although metals in proteins do not follow the rules found for inorganic compounds precisely, they show similar tendencies.[1,34] In proteins, the metal site geometry and specificity depends not only on the number of potential ligands, their stereochemical arrangement, and the relative sizes of the metal ion,[15] but also on the noninteracting secondary shell chemical groups.[19] Therefore, the protein environment, including local charges on the protein and conformational features such as helical dipoles, influences the metal site geometry and activity.[35]

Figure 1 shows examples of a few metal coordination complexes: Zn^{2+} is well-known for its role in "zinc-finger motifs"[36] and can be coordinated by nitrogen atoms present in His imidazole rings[37,38] (see Figure 1 A and Sections 3 and 4). The ability of Cu^{2+} to form strong bonds with its ligands has been employed for building biogenic materials, such as the abrasion resistant, strong jaws in *Glycera* worm (see Section 3).[39] The redox characteristics of iron ions are harnessed in the electron transport chain in heme proteins such as cytochromes as well as iron–sulfur proteins,[40] but it also catalyzes the formation of covalent cross-links based on amino acid side chains (e.g., DOPA).[41,42] The ability of Fe^{3+} (and occasionally V^{3+}) to form complexes with catechol moieties of exceptionally high stability is exploited by bacteria in siderophores, which scavenge Fe in metal-scarce environments[43] and also as load-bearing cross-links in the mussel byssus (see Sections 5 and 6; Figure 1 B). Whereas

Mg^{2+} mainly forms octahedral complexes, Ca^{2+} is able to bind a larger number of ligands with irregular geometry and fluxional behavior, thus making it a preferable ion when coordinative flexibility is required for the catalytic mechanism[44,45] (see Figure 1C).

In addition to their important role for the stabilization of secondary and tertiary protein structures, the aforementioned properties of metal–protein interactions are extensively exploited to promote the self-assembly of proteins into larger complexes.[15,46,47] Some of these metal-mediated assemblies occur naturally, such as the amyloid formation associated with certain neurodegenerative diseases[48] and virus capsid assembly.[9,49] In other cases the directionality, selectivity, and strength of protein–metal interactions is harnessed in technological applications to artificially induce assemblies, e.g., for catalysis, sensing, and pharmaceutical industries.[46] Additionally, these interactions are utilized to obtain a variety of mechanical properties in biogenic materials depending on the intended function, ranging from structural scaffolds to gel-like adhesives.

There is relatively little systemized knowledge on biogenic metallopolymers across phyla. However, there are several well-studied examples into which considerable work has been invested, including the mussel byssus,[4,50,51] hard biting parts of arthropods and annelids,[52–54] and adhesives used by sandcastle worms (*Phragmatopoma sp.*)[55,56] and terrestrial gastropods.[57] From these studies, a mechanistic understanding of how nature builds these materials and the importance of protein–metal interactions for their function is emerging. In the present review, we focus on four examples of mechanical functionalities influenced by the presence of metallic ions in extracellular protein-based materials with a specific focus on the metal-dependent mechanisms, while highlighting the need for a deeper investigation of the relationships between structure, composition, processing, and function (see Table 1). Such studies have a clear potential to influence the growing field of bioinspired metallopolymers;[4,5,11,12,58–62] however, it is important to note at this point that biological materials are not "optimized" as is often asserted. Rather, due to the manifold environment-specific physical pressures faced by a particular organism, the biological materials that they depend on for survival often represent a compromise that addresses multiple functions simultaneously. For example, a bone must at once provide load-bearing support for the organism, provide a store of calcium in the body, and in many bone types serve as a factory for blood cells.[63] Thus, it is more accurate to say that biological materials offer a multifunctional solution that suffices to simultaneously address several adaptive challenges faced by the organism. That said, the performance of biological materials is often superior in certain respects to the current state of the art in synthetic materials and, additionally, biological materials are formed as a rule under environmentally benign conditions.

3. Hard and Stiff, Unmineralized Structures

The use of metal ion cross-linking for hardening the tips and edges of specialized cuticular tools such as mandibles, stingers, ovipositors, and claws is known to occur in at least two phyla: arthropods and annelids (Figure 1A, Table 1). These tools fulfil a range of mechanically demanding functions such as stinging, venom injection, drilling (for laying eggs or feeding), cutting, scratching, and crushing for feeding purposes.[53,54,64–66] The metal-dependent mechanical properties are comparable to those of biomineralized tissues, such as bone or dentin, but with lower material density and are superior to many synthetic polymers with comparable density.[52,67] Metal-ion fortification may occur or be absent in closely related species or even between different developmental stages of the same organism depending on their ecological niche and feeding habits.[68,69] The most commonly utilized metals are Zn, Cu, Fe, Mn, and Ca, for which colocalization is often observed between the former three and the latter pair. The reasons for metal selectivity are still not well understood, as related species may use the same or different metal ions with no apparent pattern of choice. Some species incorporate different metals into different tools[57] or even at different positions within the same tool.[53] It is now

Table 1: Overview of functional metal coordination bonds found in biological materials.[a]

	Hard and Stiff	Self-healing	Hard and Extensible	Adhesive
Materials	Arthropod and Annelid biting parts	MBT core	MBT cuticle	MBT plaque; sandcastle worm glue; slug slime
Function	Biting tool	Holdfast fiber	Protective coating	Attachment, cement, predator deterrent
Metal-dependent Material Properties	Low density combined with hardness and abrasion resistance	Mechanical energy dissipation, self-healing behavior	Abrasion resistance combined with extensibility	Underwater adhesion
Metal-Ligand	His-Zn [95], ?-Cu [39]	His-Zn, His-Cu [107]	DOPA-Fe [117]	DOPA-Fe [126]; pSer-Ca/Mg [123,138]
Ligand Content (Mol % AA per protein)	>30% [52,72]	2% total, 20% in His-rich domains [102,107]	10-15% [117]	Up to 80% (for pSer) [123]
Spatial organization/cross-link distribution	Graded distribution [39,53,73]	Anisotropic; localized in extensible domains [102,103]	Localized in hard granules [115]	Isotropic [4,123]

[a] MBT = mussel byssal thread.

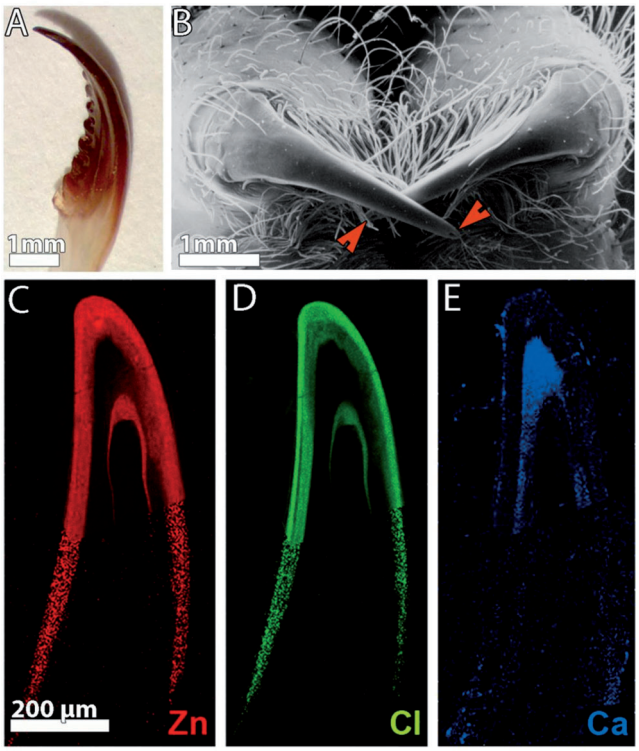

Figure 2. Hard unmineralized structures. A) *Nereis* jaw; B) spiders chelicerae fangs.[53] These tools use metal ion cross-linking to harden the tips of their structures. The red arrows mark the tips and with the venom canal. C) Metal distribution in the spider fang. Zn is found in the tip of the fang and the external layer colocalized with Cl (D), whereas Ca (E) is found in the most internal layer above the venom canal opening. Partially reprinted from [53]. Copyright 2012 WILEY-VCH Verlag GmbH & Co. KGaA, Weinheim.

accepted that genetic and cellular regulation, more than present-day environmental metal availability, control which metals are utilized.[71] The best-characterized examples in terms of their chemistry and ultrastructure are two worm jaws from *Glycera* and *Nereis* (annelida; Figure 2A) as well as the spider fang (arthropoda; Figure 2B). The degree of similarity between the three organisms is striking; however, some important differences exist, which are discussed below.

Metal ion impregnated cuticles exhibit a 1.5 to 2-fold increase in stiffness and hardness compared to similar, but metal-devoid structures with hardness increasing by a larger factor than stiffness (Table 2).[72] In ceramic materials, in which the ratio of H^3/E^2 (H refers to hardness and E to Young's modulus) is used as an estimate for abrasion resistance, this is translated into decreased susceptibility towards wear. Although the validity of this estimation was questioned in relation to tough biological materials, scratch and wear tests indicate that regions with high levels of metal ion cross-linking tend to possess enhanced wear resistance in both dry and wet states.[73] This is especially relevant bearing in mind that metal ion incorporation frequently occurs at the tips and surfaces of the functional tools. Interestingly, in the two studied examples of Zn- and Cu-rich worm jaws, the state of hydration had only little effect on the cuticle mechanical properties (in the range of 15–25 %).[72,74] This is in contrast to most organic and biological materials, whose mechanical properties are otherwise highly sensitive to hydration levels (e.g., dry insect cuticle may show 2–10-fold higher *E* and *H* values as compared to its hydrated state)[75] (Table 2).

The mechanical properties of the composite materials comprising the tools arise from hierarchical structuring as well as from the metal–protein cross-linking. In the spider fang, as in arthropods in general, chitin fibers are a central component in the cuticle, in which they function as load-bearing elements as well as form the scaffold on which the protein matrix is laid.[76,77] In *Glycera*, a melanin polymer network, accounting for 40 % of the jaw dry mass, functions similarly to chitin as a scaffold to which the proteins are bound, whereas in *Nereis*, proteins form both the fibrous and the matrix phases.[78–80] Notably, fiber arrangements with preferred orientation parallel to the jaws' long axes are found in all three and are reminiscent of fiber composites, in which the fiber orientation largely affects the (an)isotropy of their mechanical properties.[81] The secondary/tertiary structure of the matrix proteins, at least in *Glycera* jaws seems to significantly influence the mechanical properties, even in the absence of metal ions.[72] Furthermore, the matrix may also be cross-linked through the process of sclerotization by a variety of intermolecular interactions such as covalent

Table 2: Mechanical properties of some hard and stiff extracellular protein-enriched materials (measured in cross-section).

	Metal ion	Halogen	Form	D/W	H (GPa)	E (GPa)	Ref
Glycera	Cu	Cl	C.L.	D	~0.8	~10.2	a
				W	~0.6	~7.8	a
			Mineral	D	0.7^{a} - 1.3^{b}	9.2^{a} - 17^{b}	a, b
				W	0.4	0.6	a
Nereis	Zn	Cl	C.L.	D	0.7 (0.08)	10 (1)	c
				W	0.74 (0.15)	9.8 (2)	c
Nereis EDTA	-	-		D	0.38 (0.11)	6.9 (2.2)	c
				W	0.12 (0.05)	2.5 (1)	c
Spider fang	Zn	Cl	C.L.	D	0.84-1.3	20 (4)	d
	Ca	-	C.L.	D	0.7 (0.1)	14 (4)	d
Spider fang base	no metal	-	-	D	0.6 (0.2)	14 (1.6)	d

[a] Moses 2008,[74] [b] Lichtenegger 2002,[83] [c] Broomell 2008,[64] [d] Politi 2012.[53] Note: The reported mechanical properties for each material are given within a rather large range. This is well-expected in the context of biomaterials, in which microstructural and texture variations along with the presence and distribution of pore canals have a large effect on the measured values. Abbreviations: H hardness, E Young's modulus, W wet (hydrated), D dry, C.L. cross-linked. The numbers in brackets () represent standard deviation values.

bonding between modified and unmodified amino acid side chains as well as phenolic and catecholic derivatives.[82]

In the fangs of the spider *Cupiennius salei*, Zn is concentrated at the tip, with an increasing gradient towards the outer layers. It is found in tight correlation with Cl although in some regions Zn levels are increased, while Cl is almost absent (Figure 2C–E). Ca is found at the inner most layer of the tip, above the opening of the venom canal, and below the canal opening (to half way down the fang), where it decorates the outer layers of the fang. In the Zn-rich regions, traces of Fe and Cu were also observed, whereas in the Ca-rich region, traces of Mn were detected.[53] Similar ion distributions are found for Zn in *Nereis* and for Cu in *Glycera*.[39,72] Importantly, although there is a clearly established correlation between Zn and Cu incorporation and enhanced mechanical properties (H and E),[83,84] this correlation is not as apparent for Mn and Ca. However, this may be the outcome of the small number of studied materials. In the two arthropod species, in which the temporal progression of cuticle formation was studied, the incorporation of Zn precedes that of Cl (discussed further in Section 7). Other halogens, including Br or I, are also often found in these tools, but their correlation with the distribution of the metal ions is inconsistent among different materials.[85–88] Rather, they were found to be covalently bound to protein side chains, especially Tyr and His and suggested to contribute to material multifunctionality, performing mechanical,[89] protective (forming an insoluble shield), and antioxidative roles as well as stabilization against chemical or enzymatic attacks.[88] Although interesting and informative, the distribution of metal ions alone cannot account for the properties of the observed modes of fortification; thus, other parameters, such as protein composition and conformation as well as alternative cross-linking strategies (e.g., tanning) should be explored.

The composition of the protein matrix in all three cases shows remarkable similarity. Gly dominates the amino acid composition along the whole length of the structure, whereas His values increase toward the tips with as much as 25 mol% His residues.[53,72] In *Nereis* jaws and the spider fang, Ala shows an opposite trend to His and is more abundant at the base of these structures. Asp/Asn and Tyr clearly stand out in both materials, but with a more even distribution throughout the length of the structure. Proteins rich in Gly and His residues are often associated with mechanically functional structures.[52] Also, Gly- and Ala-rich domains, well-recognized from silk fibroins, are common in chitin-binding proteins from insects' cuticles.[90,91] Tyr and His are also frequently found in hard cuticles and are known to be involved in cuticular sclerotization in the absence of metal ions by covalently binding to catecholic and phenolic molecules.[88,92] In addition to naturally occurring amino acids, a multitude of PTMs have been identified in the *Nereis* jaws including various single and double Tyr and His halogenations and a variety of Tyr modifications, that is, DOPA, and di- and tri-tyrosine cross-links.[88,93]

The most imperative point to the scope of this Review is the correlation between high levels of His and the metal ions (Zn/Cu), which suggests the presence of Zn/Cu–His cross-linking in all the three cases. The nature of Zn coordination was studied using Zn K-edge X-ray absorption spectroscopy (XAS) in *Nereis* jaws and was interpreted as $ZnCl–(His)_3$.[93] A similar coordination complex is found in the Zn–insulin hexamer, in which it cross-links three monomeric insulin subunits.[94] In *Glycera*, Cu is found in two distinct forms: bound to proteins and as a chlorohydroxymineral, atacamite.[83] The mineral fraction ranges locally between 1–9 vol% and the crystallites are incorporated within protein fibers, which are themselves embedded in a Cu-cross-linked protein matrix. The Cu–protein coordination in *Glycera* is expected to involve His and perhaps Cl in a similar way as in the *Nereis* jaws; however, the occurrence of small amounts of CuI was also established from XAS measurements at the Cu K-edge. The nature of Ca and Mn incorporation in the spider fang and other arthropod structures is yet to be determined since also the amino acid compositions of the related structures are still unknown.

The mechanism of metal-ion-mediated hardening observed in biogenic tools was mainly related to the actual cross-linking of the matrix components, which primarily make up a continuous matrix and, secondly, prevent swelling by water. By replacing the metal type from Zn to Cu and Mn in sections of *Nereis* jaws, Broomell et al. showed that the hardening mechanism is not metal-specific, however the affinity and the efficacy of different metals may change considerably.[95] In that study, Mn showed the highest hardening efficacy despite exhibiting the lowest binding affinity. This was related to the ability of Mn to form complexes with higher coordination numbers, thus interacting with a larger number of protein ligands. In addition, the nature of the metal–donor interaction, that is, the degree of electron sharing, and the bonding strengths were also speculated to play a role in changing the mechanical properties.[53] The authors also showed that the displacement of water molecules from the otherwise hydrated proteins is unlikely as opposed to, for example, cuticle sclerotization.[64]

Despite fundamental differences between the structures reviewed in this section, some of the observed features seem to be universal. Whether these are a result of convergent or divergent evolution can only be determined after examination of a larger sample pool within and outside a given phyla. Nevertheless, some lessons for bioinspired material design can be obtained.

1) A structural, usually fibrous, scaffold controls the shape and structural integrity of the functional tools.
2) Biochemical and texture gradients are responsible for graded properties of the structure from tip to base.
3) Specific hardening, mainly of the outer layers as well as the tips of these tools, occurs using metal coordination chemistry, as shown by proteins enriched with His residues that bind the metal ion.

4. Self-Healing: Sacrificial Bonds and Hidden Length

The term "sacrificial bond" refers to non-covalent interactions that stabilize a folded protein structure and, under

applied load, rupture prior to the covalent bonds in the protein backbone, thus dissipating mechanical energy.[96,97] As a result of this load-induced rupture, concealed regions of the folded protein, termed "hidden length", may be extended. Thus, the combination of hidden length with sacrificial bonding provides elevated toughness and extensibility to the material, and, additionally, can lead to molecular self-repair when the material is returned to the resting state and bonds are allowed to reform.[96,97] Hydrogen bonds often serve as sacrificial bonds in protein-based systems that rely on fixed secondary structures such as β-sheet and α-helix. However, hydrogen bonds are relatively weak (0.5–5 kcal mol^{-1})[98] and do not offer much resistance to load unless combined in large numbers. This strategy is exploited in the structures of worm and spider silks, in which increased toughness is a result of the β-sheet nanocrystalline structure[99] and in materials comprised of α-helical proteins such as hair keratin, hagfish slime, and marine snail egg cases.[100] More recently, it was discovered that protein–metal interactions can also serve as reversible sacrificial bonds, as in the case of the mussel byssus, in which they contribute to deformation and self-healing properties.[101–103] In contrast to hydrogen bonds, metal complexes have the added benefit of an increased breaking force, while still being able to reform easily following rupture. In addition to the byssus, sacrificial metal bonds are also expected to contribute to the tough mechanical properties of the rapid-setting adhesive slimes of terrestrial slugs; however, this will be discussed at length in Section 5 on adhesives.

Many marine mussels (*Mytilus sp.*) reside in the wave crash zone in marine habitats, where water velocities can reach 25 $m s^{-1}$.[104] Mussels prevent dislodgement during wave impact by tethering to the hard substrate with numerous protein-based fibers known as byssal threads[105] (Figure 3 A). Byssal threads are morphologically and functionally divided into three distinct regions: the stem, the thread (distal and proximal regions), and the plaque. The thread consists of a fibrous core responsible for the tensile behavior and a thin

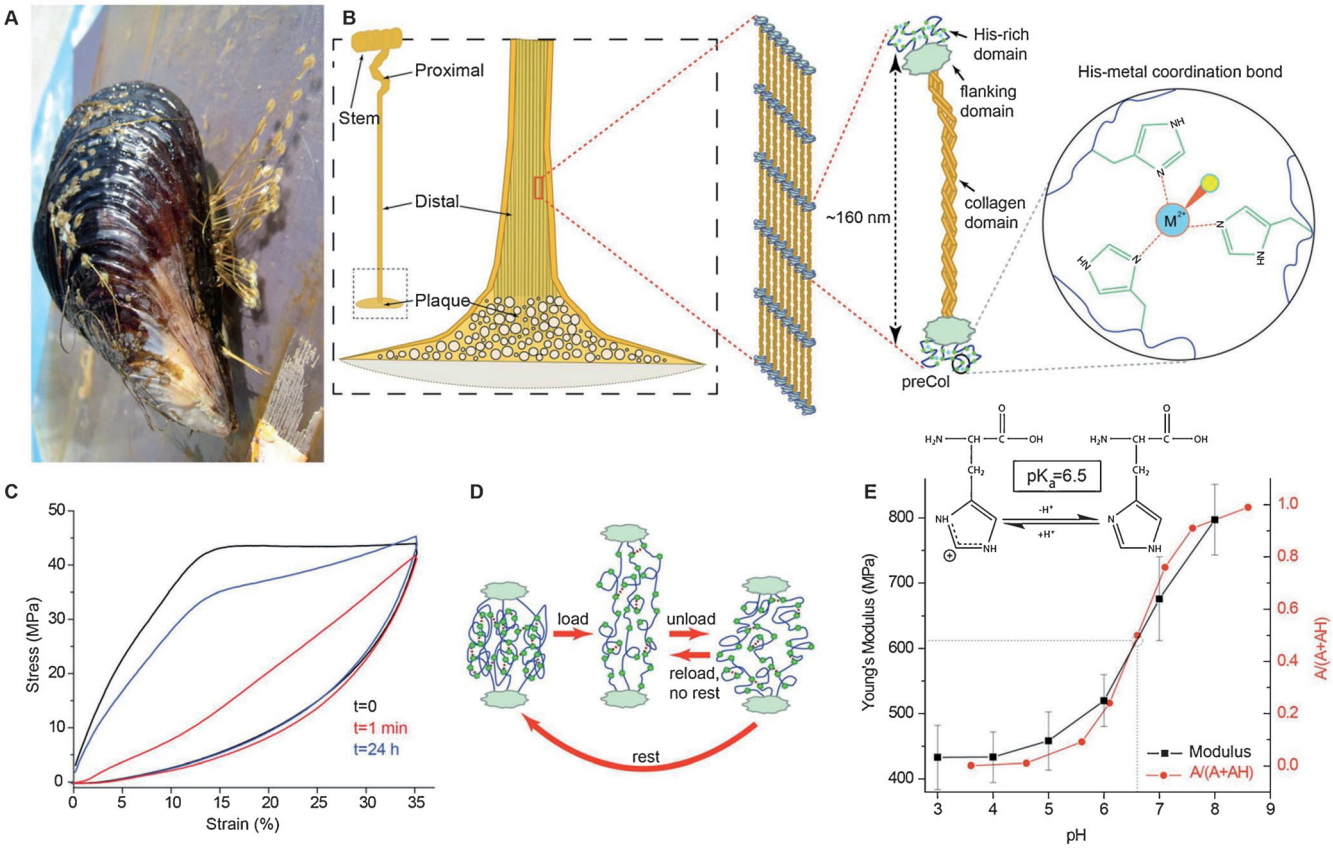

Figure 3. Role of metal coordination in the self-healing behavior of mussel byssal threads. A) Mussels use a byssus to attach to rocky surfaces at the seashore. B) Individual byssal threads are composed of proteins and subdivided into regions with specific function and properties. The distal core is composed of a highly organized semicrystalline framework made up of a protein family called preCols, which have a stiff central kinked collagen domain, highly folded flanking domains at each end of the collagen and regions rich in histidine (20 mol%)—known for its affinity for coordinating transition metal ions such as Zn^{2+} and Cu^{2+}. C) Cyclic loading of a distal mussel byssal thread ($t=0$) is followed by a loss in initial stiffness and hysteresis in a second loading cycle ($t=1$ min) immediately following the first; however, resting the thread ($t=24$ h) results in more than 80% healing of the mechanical properties.[106] D) His–metal coordination interactions in the byssus are believed to function as reversible sacrificial bonds that rupture during mechanical yield to dissipate large amounts of mechanical energy. When relaxed, the bonds do not reform in the most stable conformation, leading to a loss in stiffness. However, given time, bonds will reform leading to self-healing. E) The ability of histidine to bind metal ions is pH-dependent ($pK_a=6.5$). Soaking byssal threads in buffered solutions in the range of pH 3–8 results in a clear reduction of initial stiffness under acidic conditions in a sigmoidal fashion, which closely follows the titration curve for histidine. Adapted with permission from [102].

outer cuticle, the properties of which will be discussed in Section 5 (Figure 3B). The tensile mechanical behavior of threads is well adapted to a periodic and intense loading regime; they exhibit high stiffness, high extensibility, high hysteresis under cyclic loading, and the ability to recover initial material properties following damage sustained from material yield, that is, self-healing (Figure 3C).[106]

The main components of the thread core that determine its mechanical properties are the preCols, block copolymer-like collagenous proteins that compose approximately 95% of the distal thread core. The N- and C-terminal domains of all the preCol variants identified, invariably consist of sequences of 25–100 amino acids that contain approximately 20 mol% His residues.[102,107] It is well-documented that mussels accumulate elevated levels of transition metals such as Cu, Zn, and Fe in the byssus that are acquired through filter feeding.[108] In fact, the byssus was even employed as an environmental marker for metal contamination in polluted waters, because it was initially believed that the byssus was a depository for the harmful metals.[108] It was first proposed by Waite et al.,[107] and it is now generally accepted, that the His residues in preCols are responsible for the coordination of the incorporated transition metal ions (Cu, Zn, Ni). Furthermore, increasing evidence supports that these cross-links function as load-bearing junctions and that reversible rupture and reformation of cross-links is integral to the large energy dissipation and observed self-healing behavior in the distal region (Figure 3D). The evidence partially comes from experiments in which EDTA-mediated (EDTA = ethylenediaminetetraacetic acid) removal of metal ions resulted in a reduction of the initial modulus, hysteresis, and a loss in the ability to self-heal.[101] Moreover, low pH treatment of threads, which inhibits His–metal binding reduced the Young's modulus of the threads in a sigmoidal fashion with a halfway point at the pK_a of His and also impaired the ability to self-heal (Figure 3E).[102,103] Recently, synthetic peptides with sequences identical to regions of the mussel preCol His-rich domains were found to exhibit strong and reversible adhesive forces between peptide layers in the presence of metal ions, which were shown to originate from His–metal interactions.[109]

In addition to coordination chemistry, the hierarchical organization of protein building blocks contributes significantly to the observed mechanical behavior. Recent X-ray diffraction studies, performed during thread in situ mechanical testing, have revealed that over 98% of the distal thread extensibility arises from unfolding of the protein hidden length in the non-collagen regions of preCols, which includes the β-sheet forming flanking domains and the His-rich domains, where the metal cross-links are situated (Figure 3D).[103,110] The presence of β-sheet domains that unfold under loading, providing a store of hidden length once sacrificial bonds are ruptured, is also supported by recent spectroscopic studies.[111,112] Furthermore, the preCols were found to be organized into a semicrystalline elastic framework that recovers completely when relaxed, even after being deformed to more than 60% of the initial length, which ostensibly serves to bring the ruptured ligands into spatial vicinity necessary for reformation.[110] Complete refolding of protein structure is suggested by these investigations; however, the full recovery of mechanical properties (i.e., self-healing) requires time intervals up to several days[103,106] suggesting that the reformation of His-metal bonds into a stable topology may be a rate-limiting step. Initial modeling studies support the role of bond topology (i.e., optimal partnering of binding sites) in determining the efficacy of protein–metal sacrificial bonds;[113] however, clearly this is an area that requires further research, especially with regard to the relative contributions of the β-sheet forming domains and His-rich domains to deformation and recovery behavior. Interestingly, the rate of self-healing is species-specific,[106] suggesting that variations in the underlying protein sequences can also influence healing;[102] however, this also must be explored in more detail. While the preCols are the primary load-bearing units in the byssus, there is also a family of negatively charged matrix proteins comprising 0.5–2% of the dry mass of the distal core known collectively as thread matrix protein-1 (TMP-1), which is proposed to function as a lubricant between preCol fibrils;[114] however, their specific mechanical contribution to byssal mechanics is as of yet uncharacterized.

5. Hard and Extensible: A Network with a Heterogeneous Cross-Link Density Distribution

Thus far, we have examined examples of materials in which the self-healing functionality is dependent on the transient properties of the metal bond (usually at low metal cross-link concentrations) and those that demonstrate hardness and abrasion resistance due to increased density of protein–metal cross-links. Combining these two strategies, the mussel byssus cuticle, a thin outer coating surrounding and protecting the stretchy fibrous core (see Figures 1B and 3B as well as Table 1), exhibits hardness comparable to a typical epoxy, while maintaining the ability to extend to up to 100% strain before rupturing.[115,116] The key to this behavior lies in the granular morphology of the cuticle (Figure 4A,B), which facilitates microcracking in the matrix between the granules, thus, mitigating damage by spreading it over a larger volume.[115] The cuticle is composed primarily of a DOPA-rich protein known as mussel foot protein-1 (mfp-1) (10–15% DOPA) and a small amount of Fe^{3+} and Ca^{2+} (although the role of the latter is still not understood).[117] The co-localization of DOPA and Fe in the cuticle[117] and the in vitro demonstration that purified mfp-1 coordinates Fe ions[118] led to the hypothesis that DOPA-Fe cross-links contribute to the mechanical integrity of the cuticle. It was later confirmed, using in situ Raman spectroscopy, that DOPA side chains within the cuticle form highly stable tris complexes with Fe^{3+} (DOPA/Fe = 3:1) possessing octahedral geometry and, furthermore, that the granules are high-density centers for DOPA–Fe cross-linking, whereas the matrix possesses about half the concentration (Figure 4C,D).[50] Removal of Fe with EDTA treatment led to the loss of the DOPA–Fe Raman signal and a 50% drop in hardness.[50,119] Adhesion forces between layers of purified cuticle protein mfp-1 were measured in the absence and presence of Fe^{3+} ions using a surface

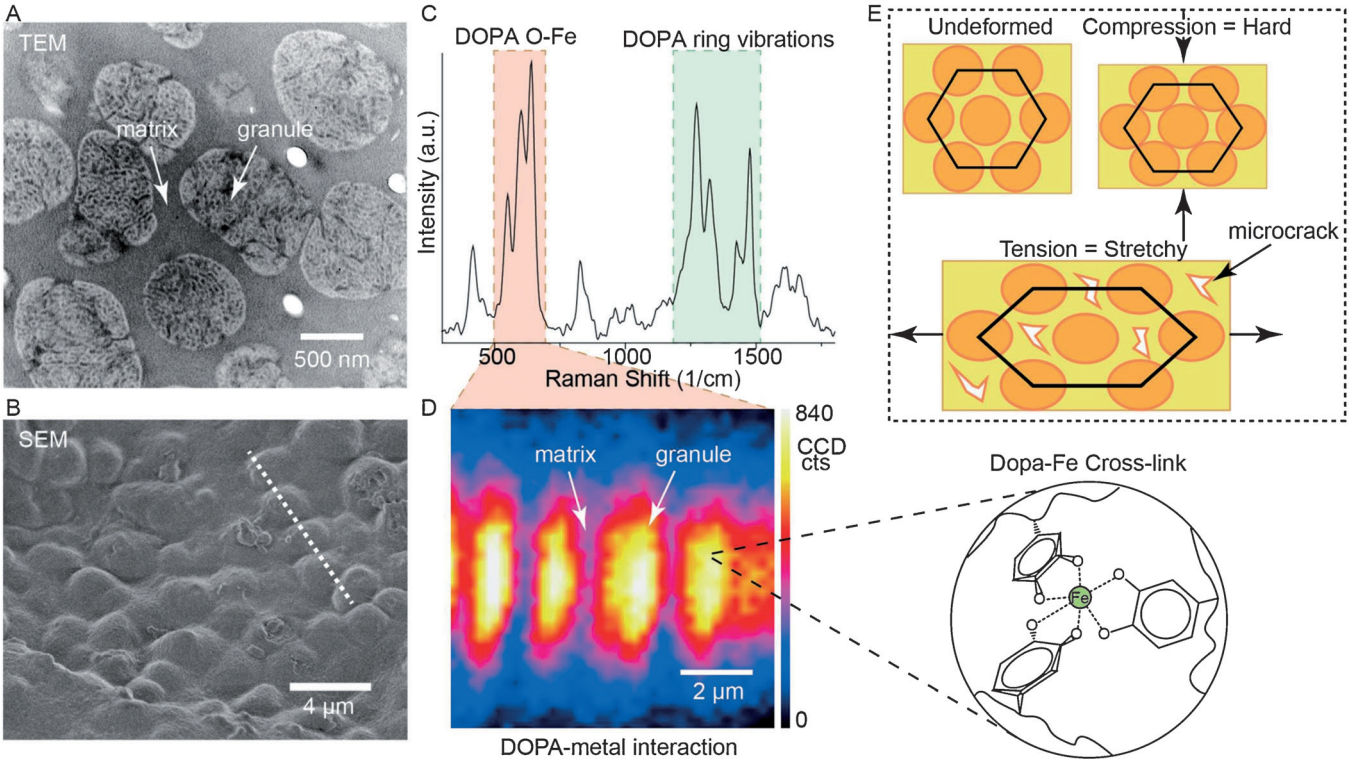

Figure 4. Role of metal coordination in the hard and extensible behavior of the mussel byssus cuticle. Mussel byssal threads have a protective outer cuticle that is as hard as epoxy, but still extensible to up to 100% strain before catastrophic cracking occurs. The cuticle consists of micron-sized granules separated by an amorphous matrix giving the surface a knobby texture as seen in A) TEM and B) SEM images. C) Raman spectroscopy of the cuticle reveals a clear signal for DOPA–metal coordination. D) A Raman depth scan across several granules (as indicated by the dashed line in (B)) integrated for the DOPA-vibrational band (490–696 cm^{-1}) indicates that although both matrix and granules contain DOPA–metal coordination, the granules contain a much higher density. E) In the current model, the heavily cross-linked granules dominate under abrasion, whereas the less cross-linked matrix deforms easily under tension, forming microcracks at high strain value, which effectively distribute the damage avoiding failure. Adapted from [50]; reprinted with permission from AAAS.

force apparatus (SFA) to examine the metal dependence of cuticle integrity. The SFA measures adhesive and repulsive forces as a function of surface separation between two initially curved elastic surfaces.[120] In these measurements, the force to separate two mica surfaces coated with mfp-1 and the adhesive contact area were measured simultaneously, and from these data, an energy of adhesion of up to 5 $mJ\,m^{-2}$ was calculated, indicating a very stable, but reversibly breakable cohesive interaction.[121]

Based on these results, a molecular level model was proposed, in which the mechanical behavior of the hard granules dominates the behavior under compressive and abrasive loading regimes, whereas the soft compliant matrix dominates the behavior under tensile loading (Figure 4E). At high strains, the metal cross-links in the matrix fail causing the formation of microcracks between granules that may be closed and healed when the thread is unloaded. Thus, this material apparently combines the hardening effect of high metal cross-link density seen in insect and arachnid biting parts with the sacrificial and healing behavior of low local densities of metal cross-links seen in the byssal thread core in order to combine the traditionally mutually excluded properties of hardness and extensibility in a single metallopolymeric material. The composite-like morphology of the cuticle reinforced by particles and the non-homogeneous distribution of metal coordination cross-linking again emphasizes the importance of a hierarchical structure in tuning the mechanical properties of biogenic metallopolymers. This is supported by the observation that thread cuticles of certain species contain no granules and fail at low strain (ca. 30%), whereas species with smaller granules (ca. 200 nm), that possess a higher matrix-granule surface area exhibit significantly higher failure strains than those with larger granules (ca. 1000 nm), while maintaining essentially the same hardness.[115,116] A deeper understanding of these underlying design principles at multiple length scales will stimulate the further development of existing mussel-inspired metallopolymeric hydrogels that exploit the DOPA-metal chemistry.[5,61]

6. Adhesives

Many organisms synthesize sticky substances that function in both permanent (e.g., barnacles, mussels, boston ivy) and temporary (e.g., limpets, marsh periwinkles, sea stars) surface attachment, as cement in composite structures (e.g., sandcastle worms), as a gummy slime for capturing prey (e.g., velvet worm), or for deterring predators (e.g., slugs, snails,

frogs, sea cucumbers) (Smith and Callow, 2006 and references therein). Among the most striking and studied properties of biological adhesives is their ability to form strong, nonspecific underwater attachments to a variety of surfaces. It is all the more impressive in marine environments, in which successful adhesives must displace surface-absorbed water molecules, ions, and larger biomolecules.[123] These challenges are well-known to developers of industrial adhesives, and thus, biological adhesion, as exemplified here in the mussel byssus attachment plaque and sandcastle worm cement, has recently attracted vast interest for the potential to inspire reliable underwater adhesives and surgical glues[4,123] as well as for combating biofouling in aquatic environments.[124] A brief survey of the diverse attachment strategies found in nature shows an impressive variability in factors influencing adhesion and cohesion such as surface compatibility, adhesion strength, morphology, and chemistry.[122] In spite of this diversity, there are several important structural and compositional commonalities recurrent in biological adhesives that are worth noting, including utilization of protein mixtures, wide use of PTMs such as DOPA and phosphoserine, and as pertains to this Review, the presence of protein–metal interactions. In this section, we focus on four examples from nature: the mussel byssus, sandcastle worm cement, caddisfly silk, and slug slime, and explore their similarities and differences in order to provide insight into the role of metal in influencing the biological adhesive behavior.

As introduced in the previous two sections, mussels survive in wave-swept marine habitats on account of their byssus attachment. Adhesion to intertidal surfaces is mediated by the byssus plaque, a protein-based disc-like structure with a foamy morphology into which the thread core fibers are anchored (Figure 3B). Similarly, the marine polychaete *Phragmatopoma californica* (commonly known as the sandcastle worm) uses a foamy proteinaceous cement to glue sand and shell debris together to build colonial tube-like enclosures from which they draw their name[125] (Figure 1C). In the case of the sandcastle worm tubes, it was proposed that the foamy structure of the adhesive cement additionally contributes to the toughness of the overall tube structure and increases cement deformability, facilitating the dissipation of mechanical energy imposed by crashing waves.[125] In addition to the morphological similarities, both the byssal plaque and *Phragmatopoma* cement are comprised of numerous protein components rife with post-translationally modified amino acids including DOPA, pSer, and hydroxyarginine, which have been implicated in the adhesive function.[4,123] More specifically, the byssus plaque is composed of a group of at least six proteins known collectively as the mussel foot proteins (mfps) that are characterized by tandemly repeated consensus sequences, basic isoelectric points (pI), and elevated DOPA content[4] (Figure 5A). The cement of the sandcastle worm also consists of a mixture of three major protein components, two of which possess elevated DOPA content (7–10 mol%) and basic pI values (Pc-1 and -2) and

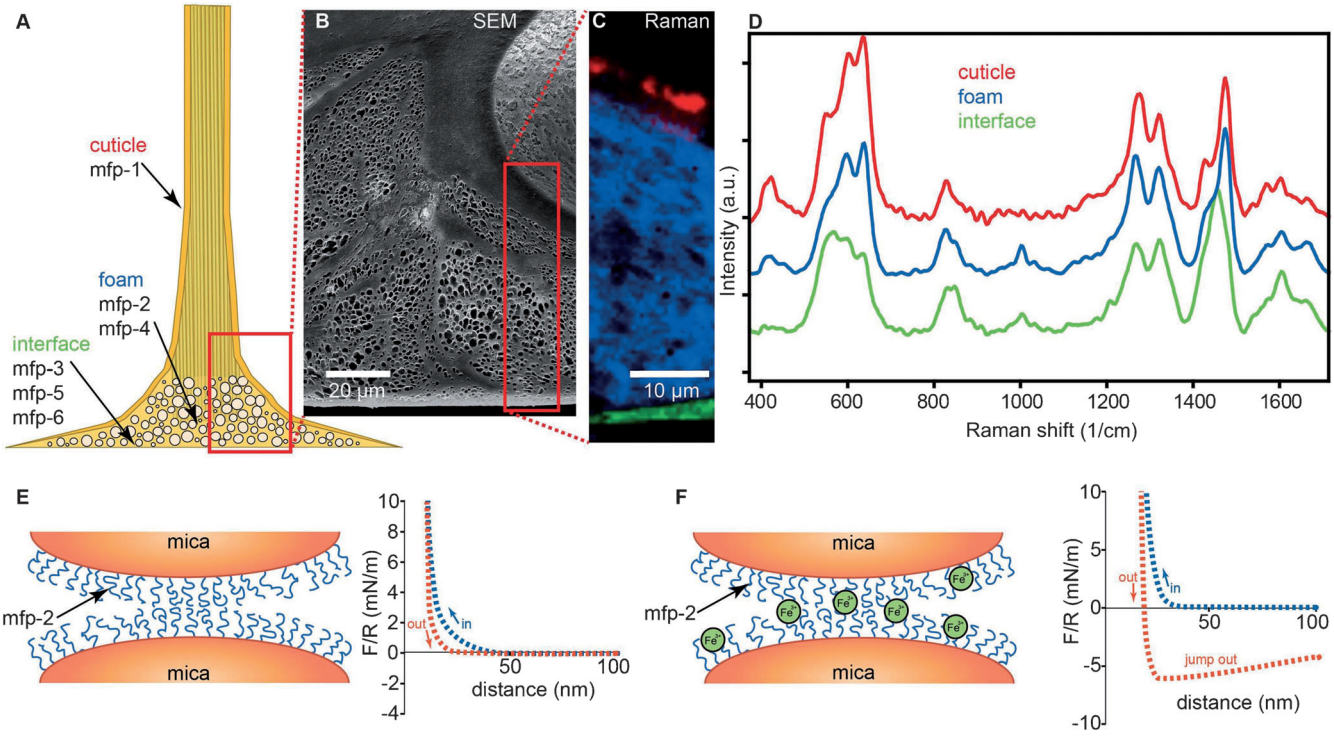

Figure 5. Role of metal ions in the adhesives plaque of the mussel byssus. A) The adhesive plaque is a complex foamy attachment structure with various DOPA-rich proteins (mfps) localized at particular regions. B) SEM of the foamy structure and sticky interface of the plaque. C and D) Raman spectroscopic imaging shows different local DOPA–metal coordination spectra (D) with the colors of the traces corresponding to the average signal from the different regions in (C). E) Surface force apparatus (SFA) measurements show no interaction forces between layers of mfp-2 in the absence of metals and high forces in the presence of metal ions (F). Figure adapted and redrawn from [126].

the third, Pc-3, with a highly acidic pI due to the presence of more than 80 mol% pSer.[123] Whereas the byssal plaque is enriched in Fe^{3+} ions,[126] the *P. californica* tube cement contains an elevated content of Mg^{2+} and Ca^{2+}.[55,56] Below, we discuss structure–function relationships inherent in each material.

At seawater pH, the two oxygen atoms of the DOPA side chain can form highly stable bidentate chelate complexes with a variety of transition metal ions.[127] Due to the elevated DOPA content and metal content in the mussel byssus plaque, metal coordination was initially assumed to be involved in the adhesive interaction.[118] Based on resonance Raman imaging, it was determined that the most abundant plaque protein, mfp-2 (5 mol% DOPA), which makes up the bulk of the foamy plaque interior, is indeed primarily cross-linked through tris-DOPA-Fe^{3+} interactions (Figure 5C,D).[126] Furthermore, SFA experiments demonstrated that two layers of mfp-2 interact in the presence of Fe^{3+} with interaction strength of up to 3 mJ m^{-2} (Figure 5E,F).[126] However, experiments exploring the interaction between mfp-2 and mica surfaces (to which mussel adhere strongly) showed only weak forces.[126] This led to the conclusion that the adhesion is likely to be mediated not by mfp-2, but rather by two smaller proteins identified directly at the interface between surface and plaque, called mfp-3 (20 mol% DOPA) and mfp-5 (28 mol% DOPA).[4,128] High adhesion energies were measured for mfp-3 (up to 4 mJ m^{-2})[4,129–131] and for mfp-5 (ca. 14 mJ m^{-2})[132] with various surfaces in the absence of metal ions, demonstrating that a combination of physical interactions including hydrogen bonding and hydrophobic interactions can mediate surface adhesion. However, numerous studies have demonstrated that several DOPA-rich mfps can also strongly adhere to metal-presenting surfaces (e.g., TiO_2) in a pH-dependent manner through coordination.[133,134] At low pH, DOPA is protonated and adhesion is achieved mainly by hydrogen bonding, while at pH > 5, the coordination bonding of Ti dominates as determined by Raman spectroscopy. As the pH is further increased, however, the oxidation of DOPA to its quinone form occurs, which was shown to reduce the metal binding affinity by approximately 80%.[30] At the pH of seawater (pH 8.2), however, keeping DOPA from oxidizing is quite a challenge, which the mussel has apparently overcome by including a cysteine-rich protein—mfp-6—at the adhesive interface with mfp-3 and mfp-5, whose proposed function is to maintain a locally reducing environment, thus impeding DOPA oxidation.[135,136] Conversely, DOPA oxidation coupled to the reduction of coordinated Fe^{3+} has been proposed as an adaptive mechanism leading to the spontaneous formation of covalent diDOPA cross-links that further stabilize the foamy interior of the plaque following secretion.[42,137] Similarly, the DOPA residues found in the proteins comprising the sandcastle worm cement are also proposed to participate in the curing of the cement through oxidative formation of covalent diDOPA cross-links.[125] In addition, adhesive and cohesive forces arising from pSer-mediated interactions with Mg^{2+} and Ca^{2+} are proposed to provide further integrity to the cement.[125] Indeed, when Mg^{2+} and Ca^{2+} are extracted from the cement by EDTA treatment, a notable reduction in adhesive force and mechanical integrity is observed.[138] pSer is a monophosphoester with two ionizable hydroxy groups that are both negatively charged at the pH of seawater, and thus, the interactions between pSer and Ca^{2+} and Mg^{2+} are more likely electrostatic in nature, rather than coordinative.[123,125,139] Although the main focus of the present Review is protein–metal coordination bonds, we choose to include this interesting and relevant example here.

Caddisfly silk is another noteworthy example in which pSer is proposed to play both a structural and adhesive role. The *Trichoptera* silks are composed of heavy chain H-fibroin and light chain L-fibroin, similarly to their terrestrial relatives. The H-fibroin is comprised of alternating stretches of positively charged Arg-rich blocks and negatively charged pSer-rich blocks.[140] The ampholytic character of caddisfly H-fibroin leads to the formation of complex coacervates during the silk formation stage[141] (discussed in Section 7). The negatively charged phosphates are proposed to interact with Ca^{2+} ions creating intra- and intermolecular bridges that promote subsequent folding into rigid domains similar to β-crystalline regions in spider and silkworm silks.[142,143] Accordingly, the presence of Ca^{2+} has been shown to play a crucial role in the structural and macroscopic mechanical properties of these silk fibers.[144] For example, removal of metal ions by chelation with EDTA resulted in a 20% decrease in the crystallinity of the structure as measured by wide-angle X-ray diffraction (WAXD),[142] accompanied by a drastic loss in mechanical integrity.[144] Notably, soaking EDTA-treated threads with Ca^{2+} was sufficient to induce full recovery of mechanical properties.[144] It is worth noting that pSer is also found in the mussel adhesive mfp-5, which contains eight Ser residues that can be variably phosphorylated.[145] Although the exact role of pSer in the mussel plaque is yet to be established, the strong, but reversible interaction between mfp-2 and mfp-5, may hold some clue since mfp-2 is known to bind Ca^{2+} ions through a specific calcium-binding domain.[145]

The glue produced by terrestrial gastropods (i.e., slugs) significantly differs in its composition and structure from the underwater adhesives produced by marine and fresh-water organisms. The primary functional requirement of slug glue is a combination of rapid setting with strong adhesion and cohesion since its function is to deter the predator just long enough for the snail to escape. The highly hydrated glues (ca. 95% water) produced by the terrestrial slug *Arion subfuscus*, the land snail *Helix aspersa*, and the marsh periwinkle *Littoraria irrorata* are gel-like materials with high adhesive and cohesive strength consisting of a mixture of different proteins, carbohydrates, and ions.[97,146,147] The limpet adhesive gel, for example, possesses an adhesion strength of 200–500 kPa,[146] whereas *A. subfuscus* glue can resist stresses of up to 100 kPa.[122] To put this into perspective, typical synthetic adhesives are in the range of 1000–8000 kPa.[148] The key structural feature of gastropod adhesive gels is the presence of glue-specific proteins not present in other forms of secretions they produce (Figure 6A).[147] The glue-specific proteins typically have acidic pI values, a large proportion of charged and polar amino acids and they range in mass from a 14 kDa slug glue protein to a 118 kDa protein in limpet glue (Figure 6B). In addition to proteins, the glue of *A. subfuscus*

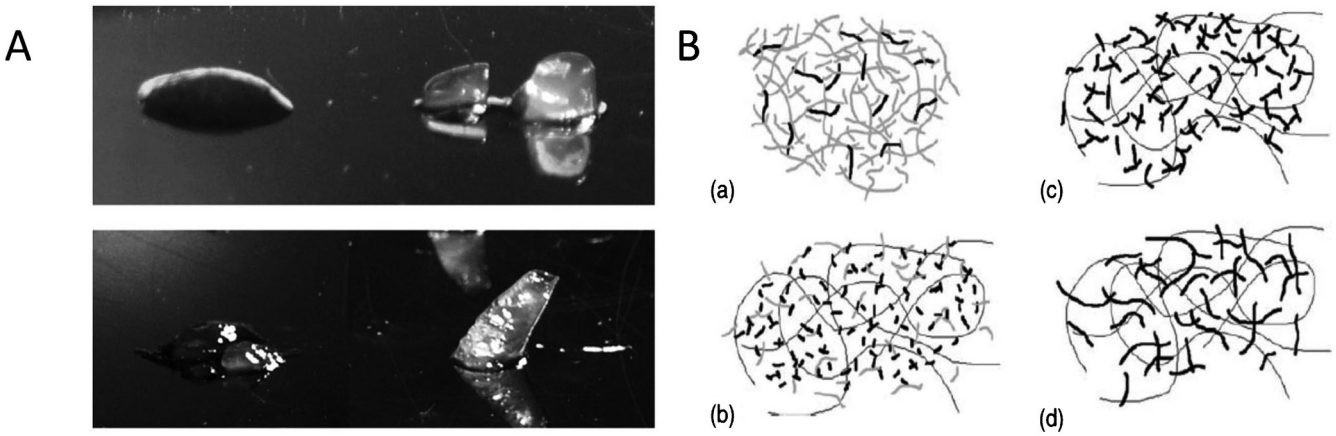

Figure 6. Properties and formation of gel-like adhesives. A) Examples of the qualitative effect of glue proteins from *L. irrorata* on gel mechanics. Samples were mixed in a microcentrifuge tube and poured or scooped out. Samples with glue proteins (0.5–1 mg mL^{-1}) are on the right (adhesive). Samples with the same concentration of BSA are on the left (control). Upper panel: 0.6% agar; lower panel: 2% polygalacturonic acid. Reprinted with permission from [147]. B) Schematic illustrations of the relative size and abundance of the components of adhesive gels from: a) the limpet *L. limatula*; b) the periwinkle *L. irrorata*; c) the slug *A. subfuscus*; and d) the land snail *H. aspersa*. Polymers of roughly 1000 kDa or larger are drawn as thin black lines, smaller proteins (10–200 kDa) are drawn as thicker lines, with glue proteins in black and other proteins in gray. The size of the polymers and relative amounts of each are depicted to scale using data from [97,146,147]. Reprinted from [57] with kind permission from Springer Science and Business Media.

contains quantities of Zn, Fe, Cu, Ca, and Mn that are significantly elevated above those detected in the local environment.[149] Currently, researchers are still attempting to determine whether the metals directly participate in cross-linking or, perhaps, participate in the catalytic formation of covalent cross-links. Although there is still no clear answer, the most prominent model suggests that the primary cross-links controlling gel stiffening involve direct linkages between Ca^{2+} ions and the glue proteins, supplemented by the cross-links formed by oxidized amino acid side chains.[149–151] Several possibilities have been raised regarding the relative contribution of direct cross-links and metal-mediated ones to the properties of the glue, including inter- and intramolecular cross-linking, mediation of polysaccharide–protein cross-linking, and stabilization by electrostatic interactions.[150] The highly redox-active Cu and Fe ions are presumed to be responsible for the aforementioned protein oxidation; however, the role of Zn ions, also present in significant amounts, is unclear, since it does not seem to contribute to glue stiffening.[150] One possibility is that Zn^{2+} inhibits oxidative cross-linking by replacing redox-active metals such as Fe and Cu. In fact, the exact role of all three metals remains uncertain, because experimental results showed no significant change in glue properties when treated with chelating agents such as deferoxamines.[149] There are several additional possible models discussed by Braun et al.;[150] however, it is clear that the existence of molecular information such as sequences for the glue-specific proteins as well as all the other proteins constituting the slug glue could significantly enhance the understanding of the processes involved.

7. Processing and the Importance of Multiscale Organization

The preceding examples indicate that it is not just the presence of metals and ligands that determines the material properties. Rather, we see repeatedly that factors such as spatial localization of the bonds within the hierarchical structure of the material, the localization of protein–metal linkages within that structure, the relative density of protein–metal cross-links, and the metal–ligand combination all contribute to the functional properties of the materials. Thus, these factors must be considered when hoping to mimic such behavior in man-made metallopolymers. Just as a house is more than the sum of its building materials, the function of hierarchically structured biogenic materials depends on the controlled organization of building blocks at multiple length scales and thus, on material processing. This is perhaps best highlighted in the cautionary tale of recombinant silk production. Despite the fact that silk protein sequences have been known for quite some time, initial attempts to reproduce recombinant spider silk with properties comparable to the natural material were largely marked by failure.[152] This difficulty was found to arise from an insufficient understanding of the intricate details involved in the storage, extrusion, and drawing occurring in the spider silk gland during the natural spinning process, combined with the complex nature of the silk proteins themselves.[153] In contrast to known synthetic polymer fiber production methods, in which physical transformation, spinning, and drawing are sequential, the natural process in a spider is rapid and concerted.[154] Following this realization, many researchers worked to improve the understanding of silk processing,[155–159] including the role of subtle transitions in pH, ion and water content, protein conformation as well as control over draw-

ing-rate, culminating in the development of biomimetic microfluidic devices capable of producing artificial silk with improved properties.[153,160]

Thus, it is hopefully evident from this review that it is not only the presence of ligand-coordinated metals that determines the observed material properties, but how they are utilized. For example, the semicrystalline arrangement of stiff and sacrificial domains in the elastic framework of byssal threads is vital in localizing damage and repairing ruptured reversible His–Zn^{2+} bonds by self-healing.[110] Likewise, laying out the chitin/melanin matrix before metal ion incorporation is integral for the performance of arthropod biting parts.[70,79] Thus, understanding of the biological control over the material production can provide important insights for the burgeoning field of bioinspired metallopolymers. Here, we highlight important processing steps in several of the best characterized systems and indicate where significant work is required, as there are still major gaps in the current understanding of the assembly for most biological metallopolymers.

Liquid crystalline mesophases and pH-triggered self-assembly: As mentioned earlier the self-healing behavior of byssal threads is very much tied to the semicrystalline organization of the primary thread protein, preCol, that superficially resembles the quarter stagger organization of type I collagen observed in a vertebrate tendon.[110] However, while tendon is assembled in a cell-assisted building process over long time scales,[161] byssal thread formation occurs in a matter of minutes as the mussel secretes the thread precursor proteins into a narrow groove running along the mussel foot where they self-assemble into a highly organized structure.[162] What, then, is the impetus driving the structural ordering of the precursors? TEM investigations of the secretory glands in the mussel foot, the organ that produces the threads, reveals that preCol precursor molecules are stored in ellipsoid secretory vesicles in a highly ordered phase resembling a smectic liquid crystal (Figure 7 A),[163] in which the long axes of the proteins exhibit preferred alignment and form layers like books on a shelf, providing organizational and orientational order. The concentration-dependent tendency for elongated biomolecules such as type I collagen, chitin and cellulose to form lyotropic LC phases in vitro is well-documented.[164,165] It was discovered that the purified preCol protein that composes the byssal thread core could be easily hand-drawn from dilute solutions into fibers possessing regular secondary structure, hierarchical organization and mechanical properties reminiscent of the native thread, thereby further supporting the presence of a transient preordered LC phase.[166,167]

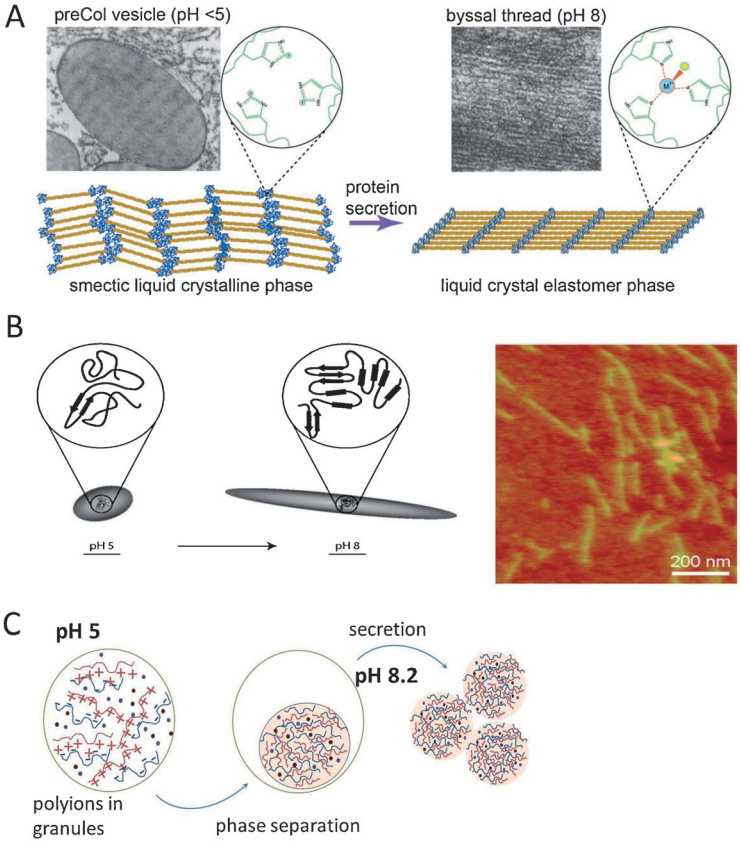

Figure 7. Processing of biological metallopolymers. A) The precursor proteins that form the core of mussel byssal threads (preCols) are stored as a smectic LC phase within vesicles at acidic pH levels prior to secretion. (TEM picture reprinted from [185], copyright (1976), with permission from Elsevier). The His residues in the preCol his-rich domains are protonated and unable to bind metal ions. Secretion results in a sudden transition to basic conditions (pH ~ 8), resulting in the deprotonation of His residues and subsequent metal binding, leading to the locking of order into a LC elastomeric fiber. (Thread TEM image reproduced with permission from [186].) B) pH effect on the structure and assembly of the main-Zn binding protein from the *Nereis* jaws (Njp-1). At low pH, the proteins exhibit globular morphology with low content of beta-sheet fold. Upon pH elevation, the protein assumes an elongated shape and the beta sheet fold fraction increases (left panel). AFM image of Njp-1 at high pH and in the presence of Zn (right panel). The protein units self-assemble to form large fibers. Reprinted with permission from [72]. Copyright 2008; American Chemical Society. C) Complex coacervation scheme in adhesive formation. From left to right: macroanion (red) and macrocation (blue), pH 5. Mg^{2+} and Ca^{2+} are pumped in to neutralize excess polyanion charges. Neutralization leads to phase separation of the coacervate from the equilibrium solution. Both phases are fluid, although the coacervate is viscous. Upon secretion into seawater at pH 8, the electrostatic interaction of Mg^{2+} and Ca^{2+} with phosphate groups becomes ionic due to low solubility, thereby increasing the viscosity of coacervate.

Utilization of a LC phase in processing is beneficial due to the pre-orientation of the precursor molecules while still allowing them to flow to the assembly site. Considering that byssal threads form in minutes, this is a major advantage for processing highly ordered fibers; however, a LC phase is useless as a load-bearing material; at some point the order of the precursor proteins must be solidified and frozen in place. During byssal thread processing, the neutral pK_a of His (ca. 6.5) and the pH differential between the byssal secretion (pH ~ 5.8)[135] and seawater (pH 8.2) is believed to be exploited to initiate pH-triggering of self-assembly. More specifically, under acidic conditions, the majority of His residues in the terminal end of the preCols will be protonated and unable to form stable complexes with metal ions. When

the pH is raised to that of seawater upon secretion into the foot groove, the His residues become deprotonated and thus, able to form intermolecular coordinate cross-links bridging the ends of the already aligned preCols (Figure 7A). This pH-dependence was also demonstrated in vitro in the drawn fibers of purified preCols such that below pH 6, fiber formation was inhibited.[167]

The pH trigger has also been found to play a significant role in the self-assembly of the *Nereis virens* jaw protein Nvjp1, the main Zn binding protein in the *Nereis* jaws. Purified Nvjp1 is expected to constitute the major component of the jaw tip and has two variants of 35 and 38 kDa. It is especially rich in Gly (36%), His (26%), and to a lesser extent also Asp (9.3%). Using cDNA libraries, the sequences of two main variants were established and the major form was expressed recombinantly allowing extensive biochemical and structural characterization.[72] At low pH (5.5) Nvjp1 is found in a globular and largely disordered form (40% random coil configuration). Upon elevation of the pH to 8 the protein assumes a more defined secondary structure with an increased proportion of β-sheets (Figure 7B).[72] Additionally, evidence suggests that the pH shift also favors packing of the existing α helices by increasing the number of H bonds. These changes in the secondary structure are accompanied with a morphological change in which the protein becomes elongated and shows an increased tendency toward aggregation. Moderate levels of Zn ions in the solution (Zn to protein ratios of 1:5) induce the formation of large fibers (Figure 7B). Less efficient fiber formation was also observed in the presence of Na. In the presence of Zn, the fibers are typically around 400 nm (and up to 800 nm) long, whereas Na-induced fibers are usually shorter. The appearance of fibers upon Zn binding in vitro is especially interesting, as the protein in pristine *Nereis* jaws is also known to reside in a fibrous state. The protein-to-Zn ratios seem to be of pivotal importance, because any deviation in the Zn concentrations led to the formation of amorphous aggregates. Thus, pH, ionic strength, and Zn concentration are reportedly effective switches driving structural transformation and self-assembly. Although nothing is known about the formation and deposition of the protein in vivo, the suggestion was made that pH differences between the secreting gland cells, which is expected to be around 6, and the extracellular matrix, likely to be elevated, along with directed control on Zn concentration could indeed be a trigger for the transformation of the precursor protein and its Zn-mediated self-assembly.

Complex coacervation during underwater adhesive formation: Complex coacervation involves the phase separation of a dense immiscible liquid phase in solutions of mixed polyanions and polycations due to charge balancing under suitable ionic conditions. Complex coacervates have been suggested to play a key role in the formation of sandcastle worm cement, caddisfly silk, and the mussel byssus adhesive plaque (Figure 7C). A thorough examination of the role of complex coacervation in the processing of biological materials can be found in the literature;[168] here, we offer a short overview stressing the role of metal ions. Assembly through complex coacervation possesses many similarities to the previous example of liquid crystalline processing, for example, a dense liquid phase, lowered viscosity, and the potential for pH triggered curing; however, the lack of structural order and the key role of charge balancing differentiates the two processes. Although it was initially suggested that the sandcastle worm cement is formed as a complex coacervate prior to secretion, it was later determined that the highly charged polyanionic and polycationic protein species comprising the cement are secreted from separate glands and are not premixed. Nonetheless, it was suggested that pH-triggered transitions in the solubility of phosphate/Mg^{2+} or Ca^{2+} mixtures likely contribute to the curing process during secretion.[168] In the case of the mussel attachment plaque, coacervate-like phase separation observed in vitro by mixing recombinant derivatives of mussel plaque proteins (mfp-1, mfp-3, and mfp-5) with polyanions, such as hyaluronic acid, led to the proposal that plaque formation may proceed through complex coacervation.[169] Although the involvement of complex coacervation in vivo seemed unlikely at the time,[168] one of the most recent reports showed that mfp-3 is capable of self-coacervation that depends on ionic strength and pH.[170] At a pH value of ca. 7.5, protein coacervation occurs, driven by both electrostatic and hydrophobic interactions, distinguishing this protein from the only other known self-coacervating protein, tropoelastin.[170]

The formation of caddisfly silk also appears to involve complex coacervation—at least according to the current understanding of the system. As mentioned in Section 6, the primary protein building blocks comprising the adhesive silks of caddisfly larvae consist of alternating patches rich in positively and negatively charged amino acid residues, respectively.[140] Mechanical disruption of the folded protein as it traverses the narrow spinneret during the silk spinning process has been proposed to lead to the shear-induced rearrangement of the protein–metal interactions, leading ostensibly to a coacervate-like phase separation.[141] In spite of an incomplete understanding of the natural systems, researchers have already drawn inspiration and adapted the general principles underlying the complex coacervation-driven formation of underwater glues to create bioinspired adhesives, for example.[171–175]

Cellular processes and assembly: Some understanding regarding the incorporation of Zn and Mn in cuticular tools of arthropods was gained from the studies of Schofield and coworkers on ants and scorpions.[54,70] The time of metal deposition in both organisms was determined by mapping Zn, Mn, Ca, and Cl in the whole organism (ants) and in the cuticular tools (scorpions) at different stages of cuticle formation. In both arthropod species, despite their relatively distant phylogenic relation, the observed sequence of metal deposition was very similar. Surprisingly, the metal ions are incorporated days after the cuticle has already assumed its final shape and is already heavily sclerotized, as judged by its dark color. Sclerotization in arthropods means the incorporation of phenolic and catecholic compounds that covalently bind and cross-link the protein matrix. Chronologically, Mn and Ca are incorporated before Zn, which is deposited concomitantly with Cl. From whole body measurements on ants, it was calculated that Zn incorporated in the mandibles constitutes less than 1% of the total Zn pool, suggesting that

Zn incorporation in mandibular tools does not involve a large metabolic cost. Late metal ion deposition requires an elaborate transport system in order to transport the metal ions through the already cross-linked matrix. Indeed, in the same study, the authors observed a high density of channels or nanopores ranging 5–50 nm in width, in both ant and scorpion hard parts. This channel network was not seen in other parts of the cuticles that do not incorporate metal ions. Importantly, the channels are predistributed in the tissue much before the onset of metal deposition and do not change their appearance thereafter. The authors speculated that the well-defined spacing between adjacent channels, in the order of 20 nm, is determined by the diffusion capacity of the Zn/Cl-rich solution. The nature and composition of that solution, however, is still unknown.

8. Summary and Outlook

Many biological materials feature noteworthy characteristic properties that make them attractive as models for the design of man-made materials, which is the primary justification for the fields of biomimetics and bioinspired materials. Along these lines, expanding the understanding of load-bearing protein–metal cross-linking and the associated material processing steps constitutes a promising avenue for inspiring the development of metallopolymers with enhanced materials properties and exciting technological and biomedical applications. For example, there have already been important advances in the direction of adhesives, antifouling coatings for implant devices, and even chemically driven actuators[176,177] that are inspired by the DOPA- and pSer-based metal interactions found in the mussel byssus and sandcastle worm cement.[4,123] Efforts towards generating bioinspired self-healing supramolecular metallopolymers and coatings for technical applications have also seen important advances in recent years.[5,58,61,178] In addition to drawing inspiration from the chemistry of natural materials, the development of bioinspired production processes should factor into future efforts by researchers; biological materials are produced efficiently under environmentally friendly ambient conditions with an economic use of locally abundant building materials, and when they outlive their use, they are typically biodegradable. As environmental pollution increases and natural resources dwindle, these factors become increasingly important reasons for mimicking nature.

Paradoxically, however, the closer polymer scientists move towards realizing functional bioinspired materials, the deeper biological materials scientists must delve into the finer details of the structure–function–processing relationships that define the performance of biological materials. Along these lines, there is a growing interest in understanding the underlying evolutionary and environmental constraints encountered by the biological organisms. For example, the selection process governing the metal ions detected in biological materials is likely not only due to their physicochemical properties, but also to their relative bioavailability in the environment. Based on this notion it seems that the pool of materials studied should be significantly expanded. However, up until a few years ago, discovery and identification of the players involved was highly restricted by the use of "classical" biochemical methods. Figure 8 depicts an evolutionary tree with the best-studied examples from different orders showing only a tiny fraction of studied species represented from the existing diversity. Development and integration of novel high-throughput identification techniques such as genome, tran-

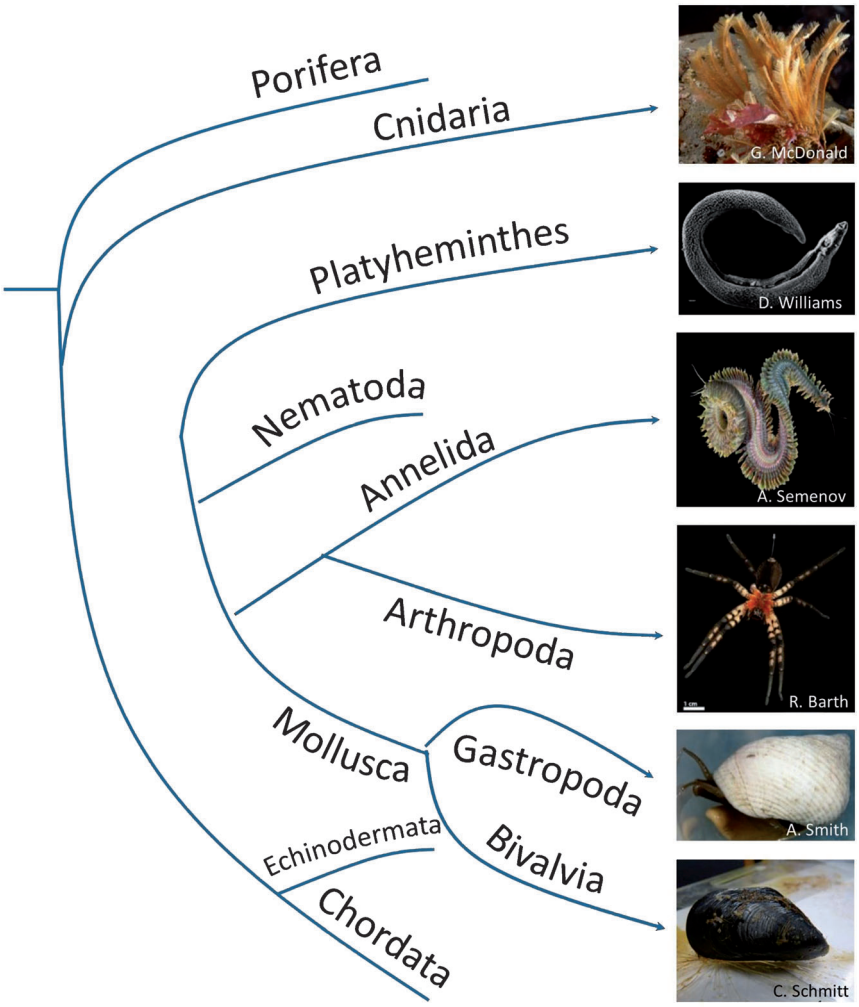

Figure 8. Schematic phylum phylogenetic tree with pictures of representative organisms from the respective phylum utilizing metal–protein bonds for structural and mechanical roles. Organisms (from top to bottom): *Aglaophenia latirostris*, *Schistosoma* parasite, *Nereis virens*, *Cupiennius salei*,[187] *Littorina irrorata*, and *Mytillus galoprovincialis*.

scriptome, and proteome sequencing will allow rapid detection of the biomacromolecules involved and reshift the focus to their characterization and processing.[179,180] Recent support for the need of greater sampling of natural materials comes from the study of perisarc in a marine hydroid (Cnidaria) that employ a previously undescribed combination of melanin, chitin, and DOPA–Fe bonds for its structure.[181] This leads back to the central idea that nature is capable of combining different types of biomacromolecules at different ratios, combinations, and hierarchical levels to achieve a great variety of mechanical functions.

We would like to thank Helmuth Möhwald for critical reading of the manuscript and for his valuable comments. We would also like to thank Gary McDonald, Alexandr Semenov, Andrew Smith, and Ralph Barth for kindly providing pictures for Figure 8.

Received: April 14, 2014
Published online: October 9, 2014

[1] R. H. Holm, P. Kennepohl, E. I. Solomon, *Chem. Rev.* **1996**, *96*, 2239 – 2314.
[2] Z. Xu, *Sci. Rep.* **2013**, *3*, 2914.
[3] M. A. Meyers, P.-Y. Chen, A. Y.-M. Lin, Y. Seki, *Prog. Mater. Sci.* **2008**, *53*, 1 – 206.
[4] B. P. Lee, P. B. Messersmith, J. N. Israelachvili, J. H. Waite, *Annu. Rev. Mater. Res.* **2011**, *41*, 99 – 132.
[5] N. Holten-Andersen, M. J. Harrington, H. Birkedal, B. P. Lee, P. B. Messersmith, K. Y. C. Lee, J. H. Waite, *Proc. Natl. Acad. Sci. USA* **2011**, *108*, 2651 – 2655.
[6] P. Fratzl, R. Weinkamer, *Prog. Mater. Sci.* **2007**, *52*, 1263 – 1334.
[7] Ref. [3].
[8] Q. Chen, N. M. Pugno, *J. Mech. Behav. Biomed. Mater.* **2013**, *19*, 3 – 33.
[9] K. I. Ishizu, H. Watanabe, S. I. Han, S. N. Kanesashi, M. Hoque, H. Yajima, K. Kataoka, H. Handa, *J. Virol.* **2001**, *75*, 61 – 72.
[10] J. D. Brodin, A. Medina-Morales, T. Ni, E. N. Salgado, X. I. Ambroggio, F. A. Tezcan, *J. Am. Chem. Soc.* **2010**, *132*, 8610 – 8617.
[11] P. X. Ma, *Adv. Drug Delivery Rev.* **2008**, *60*, 184 – 198.
[12] P. M. Favi, S. Yi, S. C. Lenaghan, L. Xia, M. Zhang, *J. Adhes. Sci. Technol.* **2014**, *28*, 290 – 319.
[13] B. D. Ratner, S. J. Bryant, *Annu. Rev. Biomed. Eng.* **2004**, *6*, 41 – 75.
[14] C. Sanchez, H. Arribart, M. M. G. Guille, *Nat. Mater.* **2005**, *4*, 277 – 288.
[15] J. A. Tainer, V. A. Roberts, E. D. Getzoff, *Curr. Opin. Biotechnol.* **1991**, *2*, 582 – 591.
[16] C. Andreini, I. Bertini, G. Cavallaro, G. L. Holliday, J. M. Thornton, *J. Biol. Inorg. Chem.* **2008**, *13*, 1205 – 1218.
[17] M. M. Harding, M. W. Nowicki, M. D. Walkinshaw, *Crystallogr. Rev.* **2010**, *16*, 247 – 302.
[18] T. Dudev, C. Lim, *Annu. Rev. Biophys.* **2008**, *37*, 97 – 116.
[19] S. Karlin, Z. Y. Zhu, K. D. Karlin, *Proc. Natl. Acad. Sci. USA* **1997**, *94*, 14225 – 14230.
[20] I. Bertini, H. B. Gray, E. I. Stiefel, J. S. Valentine, *Biological Inorganic Chemistry*, University Science Books, **2007**.
[21] J. P. Glusker, *Adv. Protein Chem.* **1991**, *42*, 1 – 76.
[22] W. N. Lipscomb, N. Sträter, *Chem. Rev.* **1996**, *96*, 2375 – 2434.
[23] M. Sono, M. P. Roach, E. D. Coulter, J. H. Dawson, *Chem. Rev.* **1996**, *96*, 2841 – 2888.
[24] J. M. Vraspir, A. Butler, *Annu. Rev. Mar. Sci.* **2009**, *1*, 43 – 63.
[25] N. Murata, *Biochim. Biophys. Acta Bioenerg.* **1969**, *189*, 171 – 181.
[26] L. L. Kiefer, S. A. Paterno, C. A. Fierke, *J. Am. Chem. Soc.* **1995**, *117*, 6831 – 6837.
[27] S. Karlin, Z. Y. Zhu, *Proc. Natl. Acad. Sci. USA* **1997**, *94*, 14231 – 14236.
[28] D. S. Auld, *Biometals* **2009**, *22*, 141 – 148.
[29] M. J. Buehler, *Nano Today* **2010**, *5*, 379 – 383.
[30] H. Lee, N. F. Scherer, P. B. Messersmith, *Proc. Natl. Acad. Sci. USA* **2006**, *103*, 12999 – 13003.
[31] W. C. Yount, H. Juwarker, S. L. Craig, *J. Am. Chem. Soc.* **2003**, *125*, 15302 – 15303.
[32] W. C. Yount, D. M. Loveless, S. L. Craig, *Angew. Chem.* **2005**, *117*, 2806 – 2808.
[33] C. L. Dupont, A. Butcher, R. E. Valas, P. E. Bourne, G. Caetano-Anollés, *Proc. Natl. Acad. Sci. USA* **2010**, *107*, 10567 – 10572.
[34] Ref. [21].
[35] T. Dudev, Y. Lin, M. Dudev, C. Lim, *J. Am. Chem. Soc.* **2003**, *125*, 3168 – 3180.
[36] A. Klug, D. Rhodes, *Trends Biochem. Sci.* **1987**, *12*, 464 – 469.
[37] P. Chakrabarti, *Protein Eng. Des. Sel.* **1990**, *4*, 57 – 63.
[38] C. Andreini, I. Bertini, G. Cavallaro, *PLoS One* **2011**, *6*, e26325.
[39] H. C. Lichtenegger, H. Birkedal, D. M. Casa, J. O. Cross, S. M. Heald, J. H. Waite, G. D. Stucky, *Chem. Mater.* **2005**, *17*, 2927 – 2931.
[40] A. Bott, *Curr. Sep.* **1999**, *2*, 47 – 54.
[41] J. Waite, *Comp. Biochem. Physiol. Part B* **1990**, *97*, 19 – 29.
[42] J. J. Wilker, *Curr. Opin. Chem. Biol.* **2010**, *14*, 276 – 283.
[43] J. Neilands, *J. Biol. Chem.* **1995**, *270*, 26723 – 26726.
[44] J. K. Jaiswal, *J. Biosci.* **2001**, *26*, 357 – 363.
[45] M. M. Harding, *Acta Crystallogr. Sect. D* **2000**, *56*, 857 – 867.
[46] E. N. Salgado, X. I. Ambroggio, J. D. Brodin, R. A. Lewis, B. Kuhlman, F. A. Tezcan, *Proc. Natl. Acad. Sci. USA* **2010**, *107*, 1827 – 1832.
[47] N. J. M. Sanghamitra, T. Ueno, *Chem. Commun.* **2013**, *49*, 4114 – 4126.
[48] B. Alies, C. Hureau, P. Faller, *Metallomics* **2013**, *5*, 183 – 192.
[49] Y.-M. Wu, C.-H. Hsu, C.-H. Wang, W. Liu, W.-H. Chang, C.-S. Lin, *Arch. Virol.* **2008**, *153*, 1633 – 1642.
[50] M. J. Harrington, A. Masic, N. Holten-Andersen, J. H. Waite, P. Fratzl, *Science* **2010**, *328*, 216 – 220.
[51] M. J. Harrington, J. H. Waite in *Fibrous Proteins* (Ed.: T. Scheibel), Landes Bioscience, Austin, **2008**, pp. 30 – 45.
[52] C. C. Broomell, R. K. Khan, D. N. Moses, A. Miserez, M. G. Pontin, G. D. Stucky, F. W. Zok, J. H. Waite, *J. R. Soc. Interface* **2007**, *4*, 19 – 31.
[53] Y. Politi, M. Priewasser, E. Pippel, P. Zaslansky, J. Hartmann, S. Siegel, C. Li, F. G. Barth, P. Fratzl, *Adv. Funct. Mater.* **2012**, *22*, 2519 – 2528.
[54] R. M. S. Schofield, M. H. Nesson, K. A. Richardson, *Naturwissenschaften* **2002**, *89*, 579 – 583.
[55] H. Zhao, C. Sun, R. J. Stewart, J. H. Waite, *J. Biol. Chem.* **2005**, *280*, 42938 – 42944.
[56] J. H. Waite, R. A. Jensen, D. E. Morse, *Biochemistry* **1992**, *31*, 5733 – 5738.
[57] *Biological Adhesives* (Eds.: A. M. Smith, J. A. Callow), Springer, Berlin/Heidelberg, **2006**, pp. 167 – 180.
[58] D. E. Fullenkamp, L. He, D. G. Barrett, W. R. Burghardt, P. B. Messersmith, *Macromolecules* **2013**, *46*, 1167 – 1174.
[59] E. I. S. Flores, M. I. Friswell, Y. Xia, *J. Intell. Mater. Syst. Struct.* **2012**, *24*, 529 – 540.
[60] H. Lee, B. P. Lee, P. B. Messersmith, *Nature* **2007**, *448*, 338 – 341.
[61] M. Krogsgaard, M. A. Behrens, J. S. Pedersen, H. Birkedal, *Biomacromolecules* **2013**, *14*, 297 – 301.
[62] E. N. Salgado, R. J. Radford, F. A. Tezcan, *Acc. Chem. Res.* **2010**, *43*, 661 – 672.

[63] J. Currey, *Bones*: *Structure and Mechanics*, Princeton University Press, Princeton, **2002**.
[64] C. C. Broomell, F. W. Zok, J. H. Waite, *Acta Biomater.* **2008**, *4*, 2045 – 2051.
[65] B. W. Cribb, A. Stewart, H. Huang, R. Truss, B. Noller, R. Rasch, M. P. Zalucki, *Naturwissenschaften* **2008**, *95*, 433 – 441.
[66] L. Kundanati, N. Gundiah, *J. Exp. Biol.* **2014**, *217*, 1946 – 1954.
[67] M. Erko, M. A. Hartmann, I. Zlotnikov, C. V. Serrano, P. Fratzl, Y. Politi, *J. Struct. Biol.* **2013**, *183*, 172 – 179.
[68] T. D. Morgan, P. Baker, K. J. Kramer, H. H. Basibuyuk, D. L. J. Quicke, *J. Stored Prod. Res.* **2003**, *39*, 65 – 75.
[69] J. Hillerton, J. Vincent, *J. Exp. Biol.* **1982**, 333 – 336.
[70] R. M. Schofield, M. Nesson, K. Richardson, P. Wyeth, *J. Insect Physiol.* **2003**, *49*, 31 – 44.
[71] B. W. Cribb, A. Stewart, H. Huang, R. Truss, B. Noller, R. Rasch, M. P. Zalucki, *Naturwissenschaften* **2008**, *95*, 17 – 23.
[72] C. C. Broomell, S. F. Chase, T. Laue, J. H. Waite, *Biomacromolecules* **2008**, *9*, 1669 – 1677.
[73] M. G. Pontin, D. N. Moses, J. H. Waite, F. W. Zok, *Proc. Natl. Acad. Sci. USA* **2007**, *104*, 13559 – 13564.
[74] D. N. Moses, M. G. Pontin, J. H. Waite, F. W. Zok, *Biophys. J.* **2008**, *94*, 3266 – 3272.
[75] D. Klocke, H. Schmitz, *Acta Biomater.* **2011**, *7*, 2935 – 2942.
[76] J. Hillerton, *Biology of the Integument*, Springer, Berlin/Heidelberg, **1984**.
[77] B. Bar-On, F. G. Barth, P. Fratzl, Y. Politi, *Nat. Commun.* **2014**, *5*, 3894.
[78] M.-F. Voss-Foucart, M.-T. Fonze-Vignaux, C. Jeuniaux, *Biochem. Syst. Ecol.* **1973**, *1*, 119 – 122.
[79] D. N. Moses, M. A. Mattoni, N. L. Slack, J. H. Waite, F. W. Zok, *Acta Biomater.* **2006**, *2*, 521 – 530.
[80] G. Bryan, P. Gibbs, *J. Mar. Biol. Assoc. U. K.* **1979**, *59*, 969.
[81] D. Raabe, C. Sachs, P. Romano, *Acta Mater.* **2005**, *53*, 4281 – 4292.
[82] S. O. Andersen, *Insect Biochem. Mol. Biol.* **2010**, *40*, 541 – 551.
[83] H. C. Lichtenegger, T. Schöberl, M. H. Bartl, H. Waite, G. D. Stucky, *Science* **2002**, *298*, 389 – 392.
[84] C. C. Broomell, M. A. Mattoni, F. W. Zok, J. H. Waite, *J. Exp. Biol.* **2006**, *209*, 3219 – 3225.
[85] R. M. S. Schofield, H. W. Lefevre, J. C. Overley, J. D. Macdonald, *Nucl. Instrum. Methods Phys. Res. Sect. B* **1988**, *30*, 398 – 403.
[86] A. Fontaine, N. Olsen, *Br. Columbia* **1991**.
[87] A. Edwards, *Cell Biol. Int.* **1993**, *17*, 697 – 698.
[88] H. Birkedal, R. K. Khan, N. Slack, C. C. Broomell, H. C. Lichtenegger, F. Zok, G. D. Stucky, J. H. Waite, *ChemBioChem* **2006**, *7*, 1392 – 1399.
[89] R. M. S. Schofield, J. C. Niedbala, M. H. Nesson, Y. Tao, J. E. Shokes, R. A. Scott, M. J. Latimer, *J. Struct. Biol.* **2009**, *166*, 272 – 287.
[90] S. O. Andersen, P. Højrup, P. Roepstorff, *Insect Biochem. Mol. Biol.* **1995**, *25*, 153 – 176.
[91] J. H. Willis, *Integr. Comp. Biol.* **1999**, *39*, 600 – 609.
[92] S. O. Andersen, *Insect Biochem. Mol. Biol.* **2010**, *40*, 166 – 178.
[93] H. C. Lichtenegger, T. Schöberl, J. T. Ruokolainen, J. O. Cross, S. M. Heald, H. Birkedal, J. H. Waite, G. D. Stucky, *Proc. Natl. Acad. Sci. USA* **2003**, *100*, 9144 – 9149.
[94] U. Derewenda, Z. Derewenda, G. G. Dodson, R. E. Hubbard, F. Korber, *Br. Med. Bull.* **1989**, *45*, 4 – 18.
[95] C. C. Broomell, F. W. Zok, J. H. Waite, *Acta Biomater.* **2008**, *4*, 2045 – 2051.
[96] G. E. Fantner, T. Hassenkam, J. H. Kindt, J. C. Weaver, H. Birkedal, L. Pechenik, J. A. Cutroni, G. A. G. Cidade, G. D. Stucky, D. E. Morse, P. K. Hansma, *Nat. Mater.* **2005**, *4*, 612 – 616.
[97] B. L. Smith, T. E. Schaffer, M. Viani, J. B. Thompson, N. A. Frederick, J. Kindt, A. Belcher, G. D. Stucky, D. E. Morse, P. K. Hansma, *Nature* **1999**, *399*, 761 – 763.
[98] S.-Y. Sheu, D.-Y. Yang, H. L. Selzle, E. W. Schlag, *Proc. Natl. Acad. Sci. USA* **2003**, *100*, 12683 – 12687.
[99] S. Keten, Z. Xu, B. Ihle, M. J. Buehler, *Nat. Mater.* **2010**, *9*, 359 – 367.
[100] A. Miserez, P. A. Guerette, *Chem. Soc. Rev.* **2013**, *42*, 1973 – 1995.
[101] E. Vaccaro, J. H. Waite, *Biomacromolecules* **2001**, *2*, 906 – 911.
[102] M. J. Harrington, J. H. Waite, *J. Exp. Biol.* **2007**, *210*, 4307 – 4318.
[103] M. J. Harrington, H. S. Gupta, P. Fratzl, J. H. Waite, *J. Struct. Biol.* **2009**, *167*, 47 – 54.
[104] M. Denny, B. Gaylord, *J. Exp. Biol.* **2002**, *205*, 1355 – 1362.
[105] C. Yonge, *J. Mar. Biol. Assoc. U. K.* **1962**, *4*, 113 – 125.
[106] E. Carrington, J. Gosline, *Am. Malacol. Bull.* **2004**, *18*, 135 – 142.
[107] J. Waite, X. Qin, K. Coyne, *Matrix Biol.* **1998**, *17*, 93 – 106.
[108] T. L. Coombs, P. J. Keller, *Aquat. Toxicol.* **1981**, *1*, 291 – 300.
[109] S. Schmidt, A. Reinecke, F. Wojcik, D. Pussak, L. Hartmann, M. J. Harrington, *Biomacromolecules* **2014**, *15*, 1644 – 1652.
[110] S. Krauss, T. H. Metzger, P. Fratzl, M. J. Harrington, *Biomacromolecules* **2013**, *14*, 1520 – 1528.
[111] A. Hagenau, P. Papadopoulos, F. Kremer, T. Scheibel, *J. Struct. Biol.* **2011**, *175*, 339 – 347.
[112] A. A. Arnold, F. Byette, M.-O. Séguin-Heine, A. Leblanc, L. Sleno, R. Tremblay, C. Pellerin, I. Marcotte, *Biomacromolecules* **2013**, *14*, 132 – 141.
[113] S. S. Nabavi, M. J. Harrington, O. Paris, P. Fratzl, M. A. Hartmann, *New J. Phys.* **2014**, *16*, 013003.
[114] J. Sagert, J. H. Waite, *J. Exp. Biol.* **2009**, *212*, 2224 – 2236.
[115] N. Holten-Andersen, G. E. Fantner, S. Hohlbauch, J. H. Waite, F. W. Zok, *Nat. Mater.* **2007**, *6*, 669 – 672.
[116] N. Holten-Andersen, H. Zhao, J. H. Waite, *Biochemistry* **2009**, *48*, 2752 – 2759.
[117] C. Sun, J. H. Waite, *J. Biol. Chem.* **2005**, *280*, 39332 – 39336.
[118] S. W. Taylor, D. B. Chase, M. H. Emptage, M. J. Nelson, J. H. Waite, *Inorg. Chem.* **1996**, *35*, 7572 – 7577.
[119] N. Holten-Andersen, T. E. Mates, M. S. Toprak, G. D. Stucky, F. W. Zok, J. H. Waite, *Langmuir* **2009**, *25*, 3323 – 3326.
[120] J. Israelachvili, Y. Min, M. Akbulut, A. Alig, G. Carver, W. Greene, K. Kristiansen, E. Meyer, N. Pesika, K. Rosenberg, H. Zeng, *Rep. Prog. Phys.* **2010**, *73*, 036601.
[121] H. Zeng, D. S. Hwang, J. N. Israelachvili, J. H. Waite, *Proc. Natl. Acad. Sci. USA* **2010**, *107*, 12850 – 12853.
[122] A. M. Smith, J. A. Callow, *Biological Adhesives*, Springer, Amsterdam, **2006**.
[123] R. J. Stewart, T. C. Ransom, V. Hlady, *J. Polym. Sci. Part B* **2011**, *49*, 757 – 771.
[124] J. A. Callow, M. E. Callow, *Nat. Commun.* **2011**, *2*, 244.
[125] R. J. Stewart, J. C. Weaver, D. E. Morse, J. H. Waite, *J. Exp. Biol.* **2004**, *207*, 4727 – 4734.
[126] D. S. Hwang, H. Zeng, A. Masic, M. J. Harrington, J. N. Israelachvili, J. H. Waite, *J. Biol. Chem.* **2010**, *285*, 25850 – 25858.
[127] M. J. Sever, J. J. Wilker, *Dalton Trans.* **2004**, 1061 – 1072.
[128] H. Zhao, J. H. Waite, *J. Biol. Chem.* **2006**, *281*, 26150 – 26158.
[129] Q. Lin, D. Gourdon, C. Sun, N. Holten-Andersen, T. H. Anderson, J. H. Waite, J. N. Israelachvili, *Proc. Natl. Acad. Sci. USA* **2007**, *104*, 3782 – 3786.
[130] W. Wei, J. Yu, C. Broomell, J. N. Israelachvili, J. H. Waite, *J. Am. Chem. Soc.* **2013**, *135*, 377 – 383.
[131] J. Yu, W. Wei, E. Danner, J. N. Israelachvili, J. H. Waite, *Adv. Mater.* **2011**, *23*, 2362 – 2366.
[132] E. W. Danner, Y. Kan, M. U. Hammer, J. N. Israelachvili, J. H. Waite, *Biochemistry* **2012**, *51*, 6511 – 6518.

[133] D. S. Hwang, M. J. Harrington, Q. Lu, A. Masic, H. Zeng, J. H. Waite, *J. Mater. Chem.* **2012**, *22*, 15530 – 15533.
[134] J. Yu, W. Wei, M. S. Menyo, A. Masic, J. H. Waite, J. N. Israelachvili, *Biomacromolecules* **2013**, *14*, 1072 – 1077.
[135] J. Yu, W. Wei, E. Danner, R. K. Ashley, J. N. Israelachvili, J. H. Waite, *Nat. Chem. Biol.* **2011**, *7*, 588 – 590.
[136] S. C. T. Nicklisch, J. H. Waite, *Biofouling* **2012**, *28*, 865 – 877.
[137] M. J. Sever, J. T. Weisser, J. Monahan, S. Srinivasan, J. J. Wilker, *Angew. Chem.* **2004**, *116*, 454 – 456; *Angew. Chem. Int. Ed.* **2004**, *43*, 448 – 450.
[138] C. Sun, G. E. Fantner, J. Adams, P. K. Hansma, J. H. Waite, *J. Exp. Biol.* **2007**, *210*, 1481 – 1488.
[139] P. Flammang, A. Lambert, E. Wattier, E. Hennebert, *Proc. 32nd Annu. Meeti. Adhes. Soc. Inc.* **2009**, 18 – 20.
[140] R. J. Stewart, C. S. Wang, *Biomacromolecules* **2010**, *11*, 969 – 974.
[141] N. N. Ashton, D. S. Taggart, R. J. Stewart, *Biopolymers* **2012**, *97*, 432 – 445.
[142] J. B. Addison, W. S. Weber, Q. Mou, N. N. Ashton, R. J. Stewart, G. P. Holland, J. L. Yarger, *Biomacromolecules* **2014**, *15*, 1269 – 1275.
[143] J. B. Addison, N. N. Ashton, W. S. Weber, R. J. Stewart, G. P. Holland, J. L. Yarger, *Biomacromolecules* **2013**, *14*, 1140 – 1148.
[144] N. N. Ashton, D. R. Roe, R. B. Weiss, T. E. Cheatham, R. J. Stewart, *Biomacromolecules* **2013**, *14*, 3668 – 3681.
[145] J. H. Waite, X. Qin, *Biochemistry* **2001**, *40*, 2887 – 2893.
[146] A. M. Smith, M. C. Morin, *Biol. Bull.* **2002**, *203*, 338 – 346.
[147] J. M. Pawlicki, L. B. Pease, C. M. Pierce, T. P. Startz, Y. Zhang, A. M. Smith, *J. Exp. Biol.* **2004**, *207*, 1127 – 1135.
[148] J. R. Burkett, J. L. Wojtas, J. L. Cloud, J. J. Wilker, *J. Adhes.* **2009**, *85*, 601 – 615.
[149] S. W. Werneke, C. Swann, L. A. Farquharson, K. S. Hamilton, A. M. Smith, *J. Exp. Biol.* **2007**, *210*, 2137 – 2145.
[150] M. Braun, M. Menges, F. Opoku, A. M. Smith, *J. Exp. Biol.* **2013**, *216*, 1475 – 1483.
[151] A. Bradshaw, M. Salt, A. Bell, M. Zeitler, N. Litra, A. M. Smith, *J. Exp. Biol.* **2011**, *214*, 1699 – 1706.
[152] A. Heidebrecht, T. Scheibel, *Adv. Appl. Microbiol.* **2013**, *82*, 115 – 153.
[153] M. Heim, D. Keerl, T. Scheibel, *Angew. Chem.* **2009**, *121*, 3638 – 3650; *Angew. Chem. Int. Ed.* **2009**, *48*, 3584 – 3596.
[154] F. Vollrath, *J. Biotechnol.* **2000**, *74*, 67 – 83.
[155] C. W. P. Foo, E. Bini, J. Hensman, D. P. Knight, R. V. Lewis, D. L. Kaplan, *Appl. Phys. A* **2006**, *82*, 223 – 233.
[156] F. Hagn, L. Eisoldt, J. G. Hardy, C. Vendrely, M. Coles, T. Scheibel, H. Kessler, *Nature* **2010**, *465*, 239 – 242.
[157] R. V. Lewis, *Chem. Rev.* **2006**, *106*, 3762 – 3774.
[158] F. Vollrath, D. P. Knight, *Nature* **2001**, *410*, 541 – 548.
[159] F. Vollrath, D. Porter, C. Holland, *Soft Matter* **2011**, *7*, 9595.
[160] S. Rammensee, U. Slotta, T. Scheibel, A. R. Bausch, *Proc. Natl. Acad. Sci. USA* **2008**, *105*, 6590 – 6595.
[161] F. H. Silver, J. W. Freeman, G. P. Seehra, *J. Biomech.* **2003**, *36*, 1529 – 1553.
[162] J. H. Waite, *Results Probl. Cell Differ.* **1992**, *19*, 27 – 54.
[163] L. V. Zuccarello, *J. Ultrastruct. Res.* **1980**, *73*, 135 – 147.
[164] A. D. Rey, *Soft Matter* **2010**, *6*, 3402.
[165] E. Belamie, G. Mosser, F. Gobeaux, M. M. Giraud-Guille, *J. Phys. Condens. Matter* **2006**, *18*, S115 – S129.
[166] M. J. Harrington, J. H. Waite, *Adv. Mater.* **2009**, *21*, 440 – 444.
[167] M. J. Harrington, J. H. Waite, *Biomacromolecules* **2008**, *9*, 1480 – 1486.
[168] R. J. Stewart, C. S. Wang, H. Shao, *Adv. Colloid Interface Sci.* **2011**, *167*, 85 – 93.
[169] S. Lim, Y. S. Choi, D. G. Kang, Y. H. Song, H. J. Cha, *Biomaterials* **2010**, *31*, 3715 – 3722.
[170] W. Wei, Y. Tan, N. R. M. Rodriguez, J. Yu, J. N. Israelachvili, J. H. Waite, *Acta Biomater.* **2014**, *10*, 1663 – 1670.
[171] Y. J. Oh, I. H. Cho, H. Lee, K.-J. Park, H. Lee, S. Y. Park, *Chem. Commun.* **2012**, *48*, 11895 – 11897.
[172] S. Kaur, G. M. Weerasekare, R. J. Stewart, *ACS Appl. Mater. Interfaces* **2011**, *3*, 941 – 944.
[173] H. Shao, K. N. Bachus, R. J. Stewart, *Macromol. Biosci.* **2009**, *9*, 464 – 471.
[174] H. Shao, R. J. Stewart, *Adv. Mater.* **2010**, *22*, 729 – 733.
[175] B. D. Winslow, H. Shao, R. J. Stewart, P. A. Tresco, *Biomaterials* **2010**, *31*, 9373 – 9381.
[176] B. P. Lee, S. Konst, *Adv. Mater.* **2014**, *26*, 3415 – 3419.
[177] C. E. Brubaker, P. B. Messersmith, *Langmuir* **2012**, *28*, 2200 – 2205.
[178] N. Holten-Andersen, A. Jaishankar, M. J. Harrington, D. E. Fullenkamp, G. DiMarco, L. He, G. H. McKinley, P. B. Messersmith, K. Y. C. Lee, *J. Mater. Chem. B* **2014**, *2*, 2467.
[179] P. A. Guerette, S. Hoon, Y. Seow, M. Raida, A. Masic, F. T. Wong, V. H. B. Ho, K. W. Kong, M. C. Demirel, A. Pena-Francesch, S. Amini, G. Z. Tay, D. Ding, A. Miserez, *Nat. Biotechnol.* **2013**, *31*, 908 – 915.
[180] S. W. Cranford, J. de Boer, C. van Blitterswijk, M. J. Buehler, *Adv. Mater.* **2013**, *25*, 802 – 824.
[181] D. S. Hwang, A. Masic, E. Prajatelistia, M. Iordachescu, J. H. Waite, *Acta Biomater.* **2013**, *9*, 8110 – 8117.
[182] S. Nair, T. Calderone, D. Christianson, C. Fierke, *J. Biol. Chem.* **1991**, *266*, 17320 – 17325.
[183] W. J. Ray, C. B. Post, Y. Liu, G. I. Rhyu, *Biochemistry* **1993**, *32*, 48 – 57.
[184] T. B. Karpishin, K. N. Raymond, *Angew. Chem.* **1992**, *104*, 486 – 488; *Angew. Chem. Int. Ed. Engl.* **1992**, *31*, 466 – 468.
[185] A. Bdolah, P. J. Keller, *Comp. Biochem. Physiol. Part B* **1976**, *55*, 171 – 174.
[186] L. Vitellaro-Zuccarello, S. De Biasi, A. Bairati, *Tissue Cell* **1983**, *15*, 547 – 554.
[187] F. G. Barth, *Zoology* **2002**, *105*, 271 – 285.